

INTERNAL AIRLIFT BIOREACTOR FOR GLUCONIC ACID PRODUCTION-MODELLING AND SIMULATION

A DISSERTATION

*Submitted in partial fulfillment of the
requirements for the award of the degree
of*
**MASTER OF TECHNOLOGY
in
CHEMICAL ENGINEERING**
(With Specialization in Computer Aided Process Plant Design)

By

NARENDRA AKITI



**DEPARTMENT OF CHEMICAL ENGINEERING
INDIAN INSTITUTE OF TECHNOLOGY ROORKEE
ROORKEE -247 667 (INDIA)
JUNE, 2009**

4

CANDIDATE'S DECLARATION

I hereby declare that the work which is being presented in the dissertation entitled **“INTERNAL AIRLIFT BIOREACTOR FOR GLUCONIC ACID PRODUCTION-MODELLING AND SIMULATION”**, in partial fulfilment of the requirements for the award of the degree of Master of technology in Chemical Engineering with specialization in **“Computer Aided Process Plant Design”**, and submitted to the **Department of Chemical Engineering, Indian Institute of Technology, Roorkee**, is an authentic record of the work carried out by me during the period June 2007 to June 2008, under the guidance of **Dr. RAVINDRA BHARGAVA**. The matter embodied in this work has not been submitted for the award of any other degree.


Date: 30/06/09

Place: Roorkee

A. Narendra
(NARENDRA AKITI)

CERTIFICATE

This is to certify that the above statement made by the candidate is correct to the best of my knowledge.


Dr. RAVINDRA BHARGAVA
ASSISTANT PROFESSOR
Department of Chemical Engineering
Indian Institute of Technology, Roorkee

ACKNOWLEDGEMENTS

These few lines of acknowledgement can never substitute the deep appreciation that I have for all those who supported, helped and motivated me throughout this work to take its present shape.

I am greatly indebted to my guide **Dr. RAVINDRA BHARGAVA**, Assistant Professor, Department of Chemical Engineering, IIT Roorkee, with whom this project had taken birth. I would like to sincerely acknowledge his valuable guidance and relentless support, discerning thoughts and loads of inspiration that led me forward to delve deeper into this work.

I would like to thank **Dr. I.D. MALL**, Head of the Department and **Dr. I.M. MISHRA**, DAC Chairman for providing various facilities during the course of my work.

I am highly thankful to **MATLAB**, a wonderful innovation by the **Math Works Inc** that helped me to calculate and present my results in a pleasant manner.

I do not have enough words to thank all my friends who encouraged and helped me to complete this work at the earliest.

Above all, I would like to acknowledge that the greatest was played by my parents who kept their pleasures away to educate me and who cultivated the system of values and instincts that shall enlighten my path for the life time.

(NARENDRA AKITI)

ABSTRACT

The airlift reactors have potential applications in biotechnology industries due to their simple construction and less shear stress imposed on shear sensitive cells compared with the mechanically stirred tanks.

A tanks-in-series model and axial dispersion model are applied for mathematical modelling of the unsteady state performance of a batch operation in a 4.5 dm³ internal loop airlift bioreactor for the production of gluconic acid by fermentation. Tanks-in-series model consists of a set of simultaneous (176 equations for 44 stages) first order ordinary differential equations obtained from material balances of cell mass, product, substrate and dissolved oxygen around the hypothetical well mixed stages in the bottom, riser, top and down comer sections of an airlift reactor. In axial dispersion model each zone of the reactor is modelled separately according to mixing properties within (ideal mixing or plug flow with axial dispersion). These equations are solved simultaneously using ODE solver of MATLAB.

Logistic and contoils models used for kinetics are compared for prediction of time dependent concentration profiles of biomass, gluconic acid, glucose and dissolved oxygen in an airlift reactor. Both models have been validated with experimental data of Znad et al (2004). Validated logistic and contoils models are used to predict the effect of change in initial biomass concentration (X_0) and airflow rate (Q_g), on the performance of gluconic acid production in airlift reactor. Effect of number of stages in tanks in series model and axial dissolved oxygen profile were investigated.

The model is simple enough to be used in design studies and it can be adapted to airlift system configurations and fermentation systems other than gluconic acid fermentation.

CONTENTS

	Title	Page No.
	CANDIDATE DECLARATION	i
	ACKNOWLEDGEMENTS	ii
	ABSTRACT	iii
	CONTENTS	iv
	LIST OF TABLES	vii
	LIST OF FIGURES	viii
	NOMENCLATURE	x
Chapter 1	INTRODUCTION	1
1.1	APPLICATIONS OF GLUCONIC ACID AND ITS DERIVATIVES	2
1.2	SCOPE OF THE PRESENT WORK	3
1.3	OBJECTIVES OF THE PRESENT WORK	3
Chapter 2	LITERATURE REVIEW	4
2.1	INDUSTRIAL PRODUCTION PRACTICES	4
2.1.1	Chemical Oxidation	4
2.1.2	Electrochemical Oxidation	5
2.1.3	Bio-Electrochemical Oxidation	6
2.1.4	Biochemical Oxidation	7
2.2	OPERATING PARAMETERS	9
2.2.1	Aeration Rate	9
2.2.2	Temperature and Pressure	10
2.2.3	Superficial Gas Velocity and Oxygen Mass Transfer Coefficient	10
2.2.4	Glucose Concentration	10

2.3	SUBMERGED FERMENTATION LITERATURE	10
Chapter 3	MATHEMATICAL MODEL DEVELOPMENT	16
3.1	ASSUMPTIONS	16
3.2	FORMULATION OF TANKS-IN-SERIES MODEL	17
3.3	MATERIAL BALANCES IN DIFFERENT SECTIONS OF THE ALR	19
3.3.1	Bottom Section	19
3.3.2	Riser Section	20
3.3.3	Top Section	22
3.3.4	Down Comer Section	23
3.4	KINETIC EQUATIONS	24
3.5	HYDRODYNAMIC AND MASS TRANSFER CORRELATIONS	26
3.6	INITIAL CONDITIONS	28
3.7	AXIAL DISPERSION MODEL	28
Chapter 4	SOLUTION OF THE MODEL EQUATIONS	32
4.1	MODEL EQUATIONS FOR SOLUTION	32
4.1.1	Tanks in Series Model	32
4.1.2	Equations for Axial Dispersion Model	34
4.2	KINETIC PARAMETERS	35
4.3	ESTIMATED DESIGN AND HYDRODYNAMIC PARAMETERS	36
4.4	SOLUTION SCHEME ADOPTED	37
Chapter 5	RESULTS AND DISCUSSION	38
5.1	ANALYSIS OF EXPERIMENTAL DATA	39
5.1.1	Variation of Biomass Concentration with Time	39
5.1.2	Variation of Gluconic Acid (GA) Concentration with Time	40
5.1.3	Variation of Glucose Concentration with Time	41

5.1.4	Variation of Dissolved Oxygen Concentration with Time	42
5.2	VALIDATION OF MODELS	43
5.2.1	Experimental and Predicted Biomass Concentration	43
5.2.2	Experimental and Predicted Gluconic Acid Concentration	45
5.2.3	Experimental and Predicted Glucose Concentration	46
5.2.4	Experimental and Predicted DO Concentration	48
5.3	EFFECT OF VARIATION OF PARAMETERS BASED ON MODEL PREDICTIONS	49
5.3.1	Effect of Initial Cell Mass Concentration (X_0)	49
5.3.2	Effect of Airflow Rate (Q_g)	51
5.4	AXIAL DISSOLVED OXYGEN PROFILE	53
5.5	EFFECT OF NUMBER OF STAGES ON MODEL VALIDATION	54
5.6	AXIAL DISPERSION MODEL	56
5.6.1	Experimental and Predicted Biomass, GA and Substrate Concentration	56
Chapter 6	CONCLUSIONS AND RECOMMENDATIONS	59
6.1	CONCLUSIONS	59
6.2	RECOMMENDATIONS	60
	REFERENCES	61
ANNEXURE-A	DESIGN PARAMETERS OF AIRLIFT BIOREACTOR	66
ANNEXURE-B	SIMULATION RESULTS	68

LIST OF TABLES

TABLE NUMBER	TITLE OF THE TABLE	PAGE NUMBER
3.1	Distribution of stages among sections in an ALR	18
4.1	Kinetic parameters of contoiois model	35
4.2	Kinetic parameters of logistic equation	36
4.3	Estimated design and hydrodynamic parameters	36
5.1	Variation range of parameter for simulation	38
B.1	Experimental data of bioprocess for gluconic acid production Znad et al. (2004)	68
B.2	Simulation data for gluconic acid production by tanks in series model using logistic equation	69
B.3	Simulation data for gluconic acid production by tanks in series model using contoiois equation.	70
B.4	Effect of initial biomass concentration (X_0) on biomass growth	71
B.5	Effect of initial biomass concentration (X_0) on gluconic acid production	72
B.6	Effect of initial biomass concentration (X_0) on glucose consumption	73
B.7	Effect of airflow rate on the biomass, gluconic acid and substrate concentrations at 57 h of fermentation	74
B.8	Simulation data for gluconic acid production by axial dispersion model using logistic equation	75
B.9	Effect of number of stages in tanks in series model on biomass, gluconic acid and substrate concentrations	76

LIST OF FIGURES

FIGURE NUMBER	TITLE OF THE FIGURE	PAGE NUMBER
2.1	Different types of <i>Aspergillus niger</i> micro organism	8
3.1	Schematic diagram of the tank-in-series model for the airlift bioreactor	18
3.2	Material balances in bottom section	19
3.3	Material balances in riser section	21
3.4	Material balances in top section	22
3.5	Material balances in down comer section	23
3.6	Schematic diagram of the Axial dispersion model for the airlift reactor	29
5.1	Concentration of biomass as a function of time	40
5.2	Concentration of gluconic acid as a function of time	41
5.3	Concentration of glucose as a function of time.	42
5.4	Concentration of dissolved oxygen as a function of time.	43
5.5	Cell biomass concentration profile represented by logistic equation	44
5.6	Cell biomass concentration profile represented by contoits equation	44
5.7	Gluconic acid concentration profile represented by logistic equation	45
5.8	Gluconic acid concentration profile represented by contoits equation	46
5.9	Glucose concentration profile represented by logistic equation	47
5.10	Glucose concentration profile represented by contoits equation	47

FIGURE NUMBER	TITLE OF THE FIGURE	PAGE NUMBER
5.11	Dissolved oxygen concentration profile represented by logistic equation	48
5.12	Dissolved oxygen concentration profile represented by contoits equation	49
5.13	Effect of change in initial cell mass on biomass growth by logistic equation	50
5.14	Effect of change in initial biomass concentration on gluconic acid production by logistic equation	50
5.15	Effect of change in initial biomass concentration on glucose consumption by logistic equation	51
5.16	Effect of airflow rate on the biomass concentration at 57 h of fermentation	52
5.17	Effect of airflow rate on the gluconic acid at 57 h of fermentation	52
5.18	Effect of airflow rate on the substrate at 57 h of fermentation	53
5.19	Axial variation of DO concentration in airlift bioreactor	54
5.20	Effect of number of stages on biomass concentration profile.	55
5.21	Effect of number of stages on gluconic acid concentration profile	55
5.22	Effect of number of stages on glucose concentration profile	56
5.23	Biomass concentration profiles represented by logistic equation	57
5.24	Gluconic acid concentration profiles represented by logistic equation	57
5.25	Glucose concentration profiles represented by logistic equation	58

NOMENCLATURE

Symbol	Description	Unit
A	Area of cross section	m^2
b	Backflow parameter, ration of the backflow rate to the net forward liquid flow rate	-
C	Concentration of the component (X, P or S)	g/dm^3
C_o^*	Saturation oxygen concentration	g/dm^3
C_o	Actual dissolved oxygen concentration	g/dm^3
D_{ax}	Axial dispersion coefficient	m^2/s
D_r	Riser diameter	m
k_B	Form friction loss coefficient for the bottom section	-
koc	Oxygen limitation constant, Contois model	g/dm^3
kos	Saturation constant, Contois model	g/dm^3
k_{La}	Overall oxygen mass transfer coefficient	h^{-1}
M	Number of stages in bottom, riser and top section	-
$M_{Glucose}$	Molecular weight of gluconic acid	g/mol
M_o	Molecular weight of atom of oxygen	g/mol
m_o	Maintenance coefficient of oxygen mass per cell mass per h	h^{-1}
m_s	Maintenance coefficient of glucose mass per cell mass per h	h^{-1}
N	Total number of stages in the ALR	-
P	Product concentration	g/dm^3
Pe	Peclet number	-
P_g/V	Power supply for mixing in the reactor per volume	W/m^3
Q	Volumetric flow rate of liquid phase	m^3/s
Q_g	Volumetric flow rate of air	m^3/s
Q_{lpm}	Air supply rate in liter per min	Lpm
R_C	Rate of formation of C (X,P or S)	$g/ dm^3.h$
R_{Co}	Rate of formation of oxygen	$g/ dm^3.h$
r_p	Rate of production formation	$g/ dm^3.h$

r_s	Rate of substrate formation	$\text{g/ dm}^3.\text{h}$
r_x	Rate of biomass growth rate	$\text{g/ dm}^3.\text{h}$
S	Substrate concentration	g/ dm^3
t	Time	h
T	Temperature	$^{\circ}\text{C}$
X	Cell biomass concentration	g/ dm^3
Y	Yield	-
U_g	Superficial air velocity	m/s
U_{gr}	Superficial air velocity in the riser	m/s
U_{gd}	Superficial air velocity in the down corner	m/s
V	Volume of reactor	m^3
v_{lr}	Superficial liquid velocity in the riser	m/s
v_{ld}	Superficial liquid velocity in the down corner	m/s
U_{Lr}	Linear liquid velocity in the riser	m/s
U_{Ld}	Linear liquid velocity in the down corner	m/s

Subscripts

b	Bottom	-
d	Down corner	-
g	Gas phase	-
G	Glucose	-
GA	Gluconic acid	-
i	Satge no., $i=1,2,\dots M-1,M,M+1, \dots N$	-
l	Liquid phase	-
m	Maximum	-
o	Initial value, $t=0$	-
r	Riser	-
t	Top	-
x	Biomass	-

Greek letters

μ	Specific growth rate	h^{-1}
μ_m	Maximum specific growth rate	h^{-1}

ε	Gas hold up	-
ε_{gr}	Gas hold up-in the riser section	-
ε_{gd}	Gas hold up-in the down comer section	-
α	Growth-associated product formation coefficient	-
β	Non growth-associated product formation coefficient	h^{-1}
γ	Growth-associated parameter for substrate uptake: substrate mass consumed per biomass mass grown	-
λ	Non growth-associated parameter for substrate uptake: substrate mass consumed per biomass mass grown per hour	h^{-1}
η	Parameter for oxygen uptake; oxygen mass consumed per biomass mass grown	-
ψ	Parameter for oxygen uptake; oxygen mass consumed per biomass mass grown per hour	h^{-1}

Chapter-1

INTRODUCTION

Gluconic acid ($C_6H_{12}O_7$, molecular mass 196.16) and its salts have lot of applications due to their low toxicity, low corrosivity and capability of forming water soluble complexes with divalent and trivalent metal ions (Hustede et al., 1989). These chemicals are used in pharmaceutical, food, textile, detergent, photographic, leather, biological and metal etching industries (Das et al., 1987). There are different approaches available for production of gluconic acid: Chemical, Electrochemical, Bio-electrochemical and Biochemical processes (Das et al., 1987; Kulkarni et al., 2002 and Klein et al., 2002). Fermentation is one of the dominant routes for manufacturing gluconic acid at present, although it suffers from many drawbacks, including those associated with process conditions required for the fermentation and microorganisms used, which has limited its commercial applicability. Further, the oxygen transfer from the gas phase into the liquid phase was found to be a limiting step for the bioconversion (Markos et al., 2002). For this reason, a great attention has to be paid for the optimization of the bioreactor operation (mixing, aeration and bioreactor design) in order to enhance the oxygen transfer rate and, hence, maximizing the product at optimized condition.

Different types of microbial species such as *Aspergillus niger* (Singh et al., 2001; Klein et al., 2002; Znad et al., 2004 and Mukhopadhyay et al., 2005), *Penicillium chrysogenum* (Ghose et al., 1990) and *Gluconobacter oxydans* (Velizarov et al., 1998) have been employed for gluconic acid production. In the present work *Aspergillus niger* is the selected microbial specie because it is capable of producing high activity of enzymes glucose oxidase (GOD) and catalase for gluconic acid production.

The success of the technology for biological production depends upon the well chosen process conditions, micro organisms going to be used, choice of the bioreactor that will efficiently achieve mixing and contact of gas liquid phases, behaviour of the organisms under prevailing conditions and medium components, hence from the different types of fermentation phenomena, namely (i) Surface fermentation, (ii) Submerged fermentation and (iii) Solid state fermentation, the submerged fermentation phenomena has been chosen for our present work because of advantages involved in submerged fermentation over surface and solid state fermentation. Oosterhuis et al. (1983)

investigated that submerged fermentation process is best suited for high production level and it can be modified for the continuous operation also.

1.1 Applications of Gluconic acid and its Derivatives

Applications of gluconic acid follows from its most important characteristics: it is a weak acid capable of dissolving the oxides, hydroxides and carbonates of polyvalent cations without attacking metallic or non-metallic surfaces. Gluconic acid, its lactones and salts are all destroyed effectively and quickly by biological waste water treatment processes (Hustede et al., 1989). Gluconic acid and its derivatives are used in the following applications:

1. Used as an additive in the food, beverage and pharmaceutical industries.
2. For removal of paint and varnishes without damaging underlying surfaces.
3. In textile industry, for desizing polyamide fabrics, for finishing natural cellulose fibres and to prevent iron deposition.
4. With gelatine, as sizing agent in paper industry.
5. Sodium salt as gluconate forms complexes with metal cations in alkaline solution and stability of such complexes often increases considerably with increasing pH.
6. For coagulation of soyabean protein in the manufacturing of tofu.
7. In leather industry, e.g. tanning of leather.
8. In concreting work sodium gluconate about 0.02-0.2 wt% is added to produce concrete highly resistant to frost and cracking.
9. Ionization of hydroxyl groups allowing use of sodium gluconate in washing of glass bottles.
10. Calcium gluconate is used to treat diseases caused by a deficiency of Ca in the body.
11. Iron gluconate is often used to supply iron in cases of anemia.
12. Ferrous phosphogluconate is used chemotherapeutically.
13. In removing calcareous and rust deposits from surfaces.
14. Sodium salts are used in the galvanic deposition of nickel-cobalt brazing surfaces on the aluminium or in the baths required for preparing smooth, shiny surface plating of nickel, tin and zinc.
15. In baking process, as a leaving agent.

1.2 Scope of the Present Work:

Gluconic acid is a product of multiple industrial significance because of its wide range of applications. The future of a majority of these applications depends mainly on commercial availability of gluconic acid and gluconates. According to the recent estimates, the annual worldwide production of gluconic acid is more than about 60,000 tones. Some companies, e.g. Prathsta Industries Ltd., Secunderabad, produce calcium gluconate (Source: Chemical Weekly, September, 2004) in small amount, against large requirement, using traditional chemical process. Large scale production of gluconic acid by fermentation process is not practiced in our country and is mostly imported nowadays because traditional chemical production processes give not only highly increased cost but also the poor yield and quality of the product. While opposite to this, bioconversion process for commercial scale production of Gluconic acid is potential as well as economic. This is the reason for present study to model the bioprocess to enhance the production using airlift bioreactor, which leads to develop a potential technology for economic fermentation process at large scale.

1.3 Objectives of the Present Work:

Looking at the scope for gluconic acid production by fermentation, which has tremendous potential for the country like ours. The present study for the production of gluconic acid in an airlift bioreactor has been taken up with following objectives:

1. To develop the mathematical model for the production of gluconic acid using airlift bioreactor by using Tanks in Series Model and Axial Dispersion Model.
2. To simulate the model and compare the results with results available in the literature.
3. Through simulation, to investigate the effect of variation in initial cell mass (X_0) and overall airflow rate (Q_g) on the performance in an airlift bioreactor.
4. To study the effect of number of stages on the conversion of gluconic acid, variation of dissolved oxygen concentration along the length of the airlift bioreactor.

Chapter-2

LITERATURE REVIEW

It had been observed that the production of gluconic acid is a function of reactor design, operating and kinetic parameters. This chapter of the report reviews the current status of the work done for the biotransformation process and its development for economic commercial scale production of gluconic acid with high yield.

2.1 Industrial Production Practices

Gluconic acid can be produced by different methods like chemical, electrochemical, bio-electrochemical and biological processes.

2.1.1 Chemical Oxidation

D-gluconic acid (penta-hydroxy-caproic acid) was discovered by Hlasiwetz and Habermann (1870) during the oxidation of glucose with chlorine. The catalysis generally employed in chemical oxidation have been finely divided platinum group metals suspended on activated charcoal; aluminium oxide, hydrogen peroxide, ozone and oxygen have been oxidants of choice. The economic viability of chemical catalysis is dependent largely on the activity, selectivity, lifetime, cost of the catalyst, measures required for product purification and energy demands. 'Kawaken fine chemicals company limited, Japan' prepared gluconic acid by air oxidation of aqueous solution of monosaccharide in presence of catalyst containing palladium (Pd) and selenium (Se). This reaction gave 98.5% conversion.

Park et al. (1986) obtained gluconic acid in 50% aqueous solution by treating calcium gluconate, prepared by chemical oxidation of glucose with oleum to precipitate calcium sulphate (CaSO_4), followed by passage over cation exchange resin and concentration of the resulting solution. The product was 95.6% pure. Calcium gluconate was reported to react with sulphuric acid to form gluconic acid. This was treated with ferric carbonate (FeCO_3) to form ferrous gluconate, which is used in food products for enrichment of iron.

Disadvantages of Chemical Oxidation

1. Limited specificity even under carefully controlled and optimized reaction conditions.
2. Unsatisfactory yields.
3. Undesirable by-products.
4. Difficult isolation and purification of the products.
5. Rapid decrease in the catalyst activity.
6. Need for highly purified glucose solutions.

2.1.2 Electrochemical Oxidation

Electrochemical oxidation electrolyzes a glucose solution with an insoluble anode in the presence of water-soluble iodide at a current density of 1-20 A/dm². Carbonates or hydroxides are added to neutralize the resulting acid. The product yield based on glucose is 80-97% (Muller et al., 1980).

The catalytic oxidation of glucose in alkaline solution at a gold (Au) electrode was studied by the cyclic voltameter at a rotating disk electrode as a function of glucose concentration and rotation velocity. The rate-determining step was concluded to be the transfer of electron from adsorbed carbohydrate radical species to the electrode. The mechanism was explained by a decrease in number of interactions between each glucose molecule and the catalytic hydrous 'Au' oxide as the glucose concentration was increased. Muller et al. (1980) investigated the adsorption and electro-oxidation of glucose on a smooth platinum electrode. The adsorption of glucose by Pt was accompanied by dehydrogenation of adsorbed molecules in neutral and alkaline solutions glucose electro-oxidation rates on Au were reported to considerably exceed those on 'Pt'. Pintauro et al. (1984) studied paired eletrochemical synthesis of gluconic acid and sorbitol in undivided flow cells. Reduction in energy consumption by 50% was achieved compared to the conventional synthesis. The synthesis of gluconic acid was carried out in parallel plate and packed bed cells. The optimum electrode materials and operating conditions for the synthesis were: an amalgamated zinc (Zn) cathode, graphite anode and initial glucose concentration of 0.8 mol/dm³, sodium bromide (NaBr) supporting electrolyte, electrolyte flow rate of 0.8 dm³/min and electrolyte pH of 7.

A catalyst was made by entrapping glucose oxidase in a polymeric film deposited on platinum electrode surface by anodic electro polymerization of pyrrole 0.1 mol/dm^3 in phosphate buffer containing perchlorate ions 0.1 mol/dm^3 as counter anions and glucose oxidase 1.5 g/dm^3 . The electrochemical step affected the enzymatic catalysis in two ways, the reactant oxygen was regenerated and the product, hydrogen peroxide (H_2O_2), which is glucose oxidase inhibitor, was consumed. When no potential was applied, the electrode only acted as an inert support. When a suitable potential was applied, H_2O_2 underwent oxidation at the electrode. The electrochemical step could occur throughout the polymeric structure rather than being limited to the electrode surface.

Disadvantages of Electrochemical Oxidation

Cost of the electricity is very high; in such a situation it is costly to use electrochemical method for oxidation of gluconic acid. The other disadvantages are the poisoning of the electrodes and low oxidation potentials of halogens.

2.1.3 Bio-Electrochemical Oxidation

Biocatalyst electrodes (oxidoreductase immobilized electrodes) in which the electrode behaved as a substitute for a chemical electron acceptor or donor of a oxidoreductase reaction were used in novel applications such as biosensors, bioreactors and biofuel cells. A film-coated glucose oxidase-immobilized 'Au' minigrad electrode with P-benzquinone-mixed paste and a film coated glucose oxidase-immobilized 'Pt' mesh electrode with oxygen permeable membrane were designed. These electrodes worked satisfactorily as biocatalyst electrodes oxidizing d-gluconate. Glucose was converted to gluconic acid and hydrogen by glucose oxidase from *Aspergillus niger* (Tokuji et al., 1985).

Glucose oxidase and baker's yeast invertase catalyzed the conversion of sucrose to gluconic acid, fructose and hydrogen. Finally, glucose oxidase and cellulose transformed cellulose to gluconic acid and hydrogen. Another potential source of glucose for the bio-electrochemical cell, starch was degraded to glucose by the combined action of amylase and amyloglucosidase (Laane et al., 1984).

A bio-electrochemical cell containing either glucose oxidase or xanthine oxidase with dichlorophenol indophenol as electron acceptor in one half and chloroperoxidase in

the other half of the cell was described by Laane et al. (1984). Due to the combination of chemical, biochemical and electrobiochemical reactions, specific biochemicals could be produced in the cell simultaneously and in both the compartments. Furthermore, H_2O_2 did not inactivate the oxidases in a bio-electrochemical cell and as a result, the operational lifetime of both the oxidases increased.

2.1.4 Biochemical Oxidation

The conversion of glucose to gluconic acid by biochemical methods can be classified into microbial and enzymatic routes. In microbial synthesis, the main strains used have been *Aspergillus niger*, *Gluconobacter suboxydans* and *Zymomonas mobilis*. The pathway by which gluconic acid is produced using these strains depends upon the type of strain used. Fermentation process can broadly be classified in three categories: surface fermentation, submerged fermentation and solid-state fermentation. In which submerged fermentation processes are undoubtedly the most frequently used fermentation technique, because it offers simple operation and is inexpensive to conduct with low fermenter cost etc. Although it is having some weakness too, like: limited maximum oxygen transfer rate and not always best fermentation method for all types of micro-organisms.

The present work is based on the microbial synthesis phenomena of *Aspergillus niger* using submerged fermentation.

Aspergillus niger

Aspergillus niger is economically important as a fermentation organism used for the production of gluconic acid. Currently industrial gluconic acid production by *Aspergillus niger* represents one of the most efficient, highest yield giving microorganism in use.

Fig. 2.1 shows microscopic pictures of some types of *Aspergillus niger* micro organism. The biotransformation of glucose to gluconic acid represents a simple dehydrogenation reaction without involvement of complex metabolic pathways, which is realized with a high selectivity, high rate and high yield of conversion. Gluconic acid is formed by the hydrolysis of the gluconolactone ($C_6H_{10}O_6$), the by product of the reaction

(H₂O₂) is decomposed to water and oxygen by enzyme catalysis, which is present in the living cells.

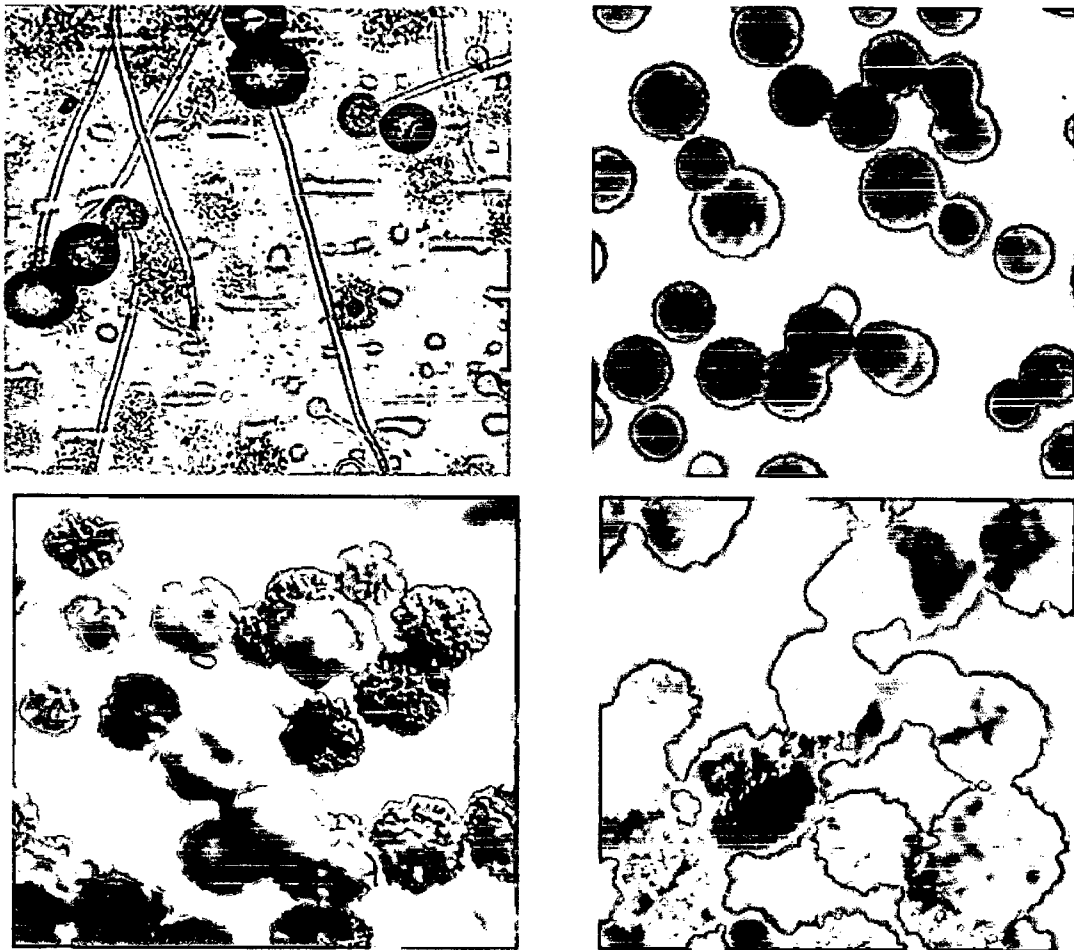
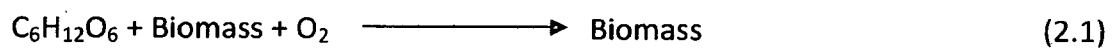


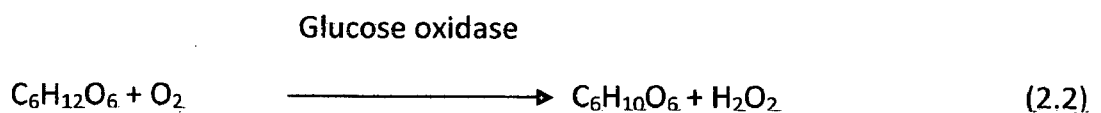
Fig 2.1 Different types of *Aspergillus niger* micro organism.

The overall reaction mechanism can be described as follows.

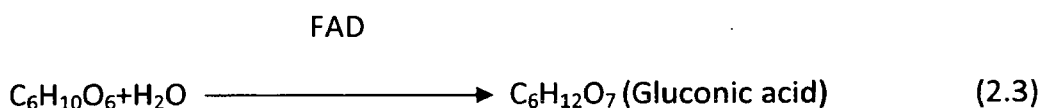
Cell Growth:



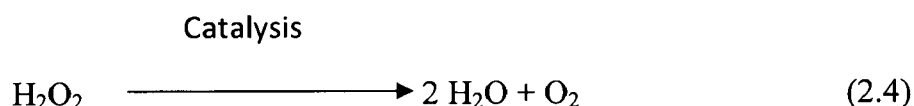
Glucose Oxidation:



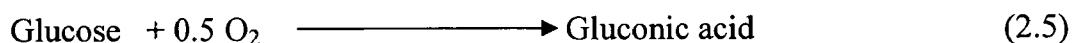
Gluconolactone hydrolysis:



H₂O₂ Decomposition:



The overall reaction is represented by:



2.2 Operating Parameters

To determine a suitable set of input operating parameters that provides an optimal set of output parameters is a major challenge, primarily due to the existence of multiple substrate, varieties of microorganisms and different design of experimental set ups. The purpose of this section is to search a suitable set of operating parameters. This task is constrained by a lack of uniformity of suitable data. The different workers proposed varying operating parameters for the submerged fermentation process. These proposed operating parameters may be used as the starting information for the bioprocess development.

2.2.1 Aeration Rate

Low solubility of oxygen in an aqueous media and the poor transport properties make the oxygen supply a rate limiting factor. The airflow should be such that it maintains the maximum oxygen concentration in the solution. The optimum range of airflow rate proposed by Znad et al., (2004) is 15 dm³/min in 10.5 dm³ internal loop airlift bioreactor operated for 57 h of batch time beyond which the process will not be economical. Das & Kundu (1987) and Markos et al. (2002) suggested about 1-1.5 vol air/vol solution per min (vvm) of air flow rate as optimum. This is equivalent to 4.5-6.75 lpm in a 4.5 dm³ reactor (size of airlift reactor used in present study).

2.2.2 Temperature and Pressure

Lantero et al. (2004) studied the effect of temperature and found that optimum temperature is 30°C. pH should be maintained 6.5 during the growth phase and at 5.5 during the production phase by addition of NaOH as used by Markos et al. (2002).

Further, the inoculation level found by Singh (2000) and Markos et al. (2002) is 2%. Antifoam addition, if required, would be about 80-120 ppm. Higher pressure increases the oxygen solubility, but operating cost goes up. So the reactor should be operated at the pressure slightly above the atmospheric pressure.

2.2.3 Superficial Gas Velocity and Oxygen Mass Transfer Coefficient

The oxygen dissolved from the liquid is used only for biotransformation of glucose to gluconic acid. Thus the oxygen transport characteristic of oxygen from gas phase to the liquid phase influences the gluconic acid production. A higher airflow rate supports a higher supply of oxygen into the bioreactor and increases the gas hold up, enhance bulk mixing and improve DO and mass transfer. Thus, the optimum value of this parameter is of prime importance.

Znad et al (2004) indicated riser superficial gas velocity as 0.0667 m/s (equivalent to 15 dm³/m) in 10.5 dm³ airlift fermenter beyond which the process may not be economic.

2.2.4 Glucose Concentration

This parameter is very conflicting as different workers proposed different values; Znad et al (2004) used a value of 200 g/dm³ in his work. Higher glucose concentration will reduce the inhibition effect of product in the solution during the fermentation of glucose.

2.3 Submerged Fermentation Literature:

Some of the reported literature is reviewed in following paragraphs.

Kawase et al. (1996) used a tanks-in-series model for mathematical modeling of the steady state performance of continuous cultures in an airlift bioreactor. The objective of his study was to investigate effects of mixing in the riser and the down comer on

microorganism growth in an airlift bioreactor for continuous culture processes. A mathematical model was developed based on a tanks-in-series model with backflow, it consist of non-linear algebraic equations. Which are material balances of micro organism, substrate and dissolved oxygen for hypothetical well mixed tanks or stages. They have been solved using Newton-Rapson technique. It was found that the down comer is a unique feature of airlift bioreactors and liquid mixing in the downcomer may significantly influence their productivity. Therefore, the recycle flow rate into the down comer is one of the important parameters for the optimum design and operation of airlift bioreactors. In this study, the airlift bioreactor was assumed to operate under isothermal conditions, as heat balances in the airlift bioreactor are not considered. A simple kinetic model proposed by monod was used in this work which is given by

$$\mu = \mu_m \frac{S}{(K_s + S)} \quad (2.6)$$

In the work of Nakao et al. (1997) an external loop airlift bubble column (ELBC), an internal loop airlift (ILBC) and a normal bubble column (NBC) were employed as promising bioreactors to carry out the immobilized glucose oxidase catalyzed oxidation of glucose with air to produce gluconic acid as a model of immobilized enzyme reactions. Optimal reactor design and operating conditions were searched for in relation to its accumulation based on the reaction kinetics and reactor sharakteristics. A useful determination of optimal operating condition was proposed for each reactor type. ILBC and NBC were found to give higher productivity and lower glucose oxidase activity decay due to their better mass transfer than ELBC.

Bioconversion of glucose to gluconic acid at low pH using *Aspergillus niger* immobilised on cellulose fabric was investigated by Sankpal et al. (1999). Glucose solution (100 kg/m³) was made to flow through capillaries of a vertical fabric support, used for immobilization and was oxidized to gluconic acid at the interface. Conditions of temperature, humidity, airflow and glucose feed rate have been optimized. The system could be run continuously for a period of 61 days utilizing the entire available glucose.

According to Jurascik et al. (2000), gluconic acid fermentation by the filamentous fungi *Aspergillus niger* belongs to aerobic fermentation with high oxygen demand. The biotransformation of glucose to gluconic acid represents a simple dehydrogenation

reaction without involvement of complex metabolic cell pathways. Which is carried out with a high selectivity, high rate and high yield of conversion.

Their study dealt with glucose-gluconic acid fermentation by *Aspergillus niger* in internal loop airlift reactors (ILALR). The fermentations were carried out in three ILALR (10.5 dm³, 40 dm³ and 200 dm³). Growth fermentations (40 dm³ and 200 dm³) were performed under constant air flow rate, and non-growth fermentations were carried out under various gas flow rates in order to study the effect of circulation velocity of the system.

In the paper of Klein et al. (2002), a glucose-gluconic acid biotransformation system was suggested with *Aspergillus niger* strain for the experimental study of oxygen transfer in bioreactors. This biosystem was used for the investigation of the effect of the flow rate and biomass concentration on the volumetric oxygen transfer coefficient in a 10 dm³ internal loop airlift bioreactor. For this purpose, the fermentation broth of the mycelial strain *Aspergillus niger* was employed, representing a three-phase system, where bubbles come in to contact with dense rigid pellets. The results showed that the presented biotransformation system could be successfully utilized for the determination of the oxygen transfer rate in internal loop airlift bioreactors.

The optimization of gluconic acid fermentation using immobilized *Aspergillus niger* on a highly porous cellulose support is described in the work of Sankpal et al. (2002). Experimental results showed the effects of variations in oxygen partial pressure, glucose concentration and biomass concentration for a continuous recirculation reactor. Levels of dissolved oxygen and glucose concentrations during fermentation significantly affected the production and fermentation time. Morphological characteristics of immobilized *Aspergillus niger* had also been investigated. Higher levels of glucose and DO enhanced the productivity of gluconic acid. They concluded that oxygen enriched air can substitute pure oxygen and reduce the fermentation period substantially.

Calcium gluconate production by *Aspergillus niger* was investigated by Tripathi et al. (2003) in shake flask, rolling shaker, airlift reactor and stirred reactor at different initial glucose concentrations. They observed that success of the technology for biological products depends on the choice of bioreactor efficiently achieving mixing and contact of liquid and gas phases. Further, it was found that high calcium gluconate production was

achieved in airlift reactor with pellet form of cell growth at moderate specific growth rate and biomass concentration, while in stirred reactor pulpy mycelial growth was obtained and hence calcium gluconate production was poor.

Response surface methodology (RSM) was applied to optimize the speed of agitation and the rate of aeration for the maximum production of glucose oxidase (GOD) by *Aspergillus niger* in the work of Liu et al. (2003). A quadratic model for GOD production was obtained. Aeration had more negative effect on GOD production than agitation. Significant negative interaction existed between agitation and aeration. The quadratic term of agitation presented significant positive effect. The fermentation kinetics of GOD by *Aspergillus niger* were also studied in a batch system. A simple model was proposed using the Logistic equation for growth, the Luedeking-piret equation for GOD production and Leudeking-piret-like equation for glucose consumption. The model appeared to provide a reasonable description for each parameter during the growth phase.

Jian-Zhong et al (2003) studied the fermentation kinetics of gluconic acid by *Aspergillus niger* in a 5 dm³ stirred tank bioreactor with a working volume of 4.0 dm³. A mathematical model was proposed using the logistic equation, which describes the inhibition of biomass on growth, to represent the behaviour of gluconic acid production in stirred tank bioreactor in batch.

$$\frac{dX}{dt} = \mu_m X \left[1 - \frac{X}{X_m} \right] \quad \text{where, } X_m \text{ is maximum cell concentration} \quad (2.7)$$

The model provided a reasonable description for each parameter during the growth phase. The evaluated value of maximum specific growth rate (μ_m) is 0.22 h⁻¹. It was found that the gluconic acid formation is strongly linearly related to cell growth and is growth-associated. X_m is taken as the experimental value for modeling.

A tanks-in-series model was applied for mathematical modelling of the unsteady state performance of a semi batch operation by Znad et al. (2004 a) in a 10.5 dm³ internal loop airlift bioreactor for the production of gluconic acid by fermentation. The kinetic model used considered the effect of two substrates (glucose and dissolved oxygen) on the growth rate.

Both the effect of airflow rate and the height of the airlift bioreactor on the gluconic acid production were investigated. The model has been validated with

experimental data. The model is simple enough to be used in design studies and it can be adapted to airlift system configurations and fermentation systems other than gluconic acid fermentation.

The model is suitable to predict the effect of airflow rate on the process. For gluconic acid fermentation an optimum range of airflow rate (9–45 dm³/min) is suitable in a 10.5 dm³ internal loop airlift bioreactor beyond which the process will not be economical. Also the effect of the bioreactor height on the axial dissolved oxygen has been predicted by the model. The shorter bioreactor, shows relatively more uniform axial DO concentrations than the longer bioreactor, where a greater variation in DO concentrations with the height was observed. The model has been tested and the values were compared with experimental data.

Zand et al. (2004 c) conducted batch fermentation of glucose to gluconic acid using *Aspergillus niger* under growth and non-growth conditions using pure oxygen and air as a source of oxygen for the fermentation in 2 and 5 dm³ stirred tank reactors. Production of gluconic acid under growth conditions was conducted in a 5 dm³ batch reactor. Production and growth rates were higher during the period of supplying pure oxygen than that during supplying air, and the substrate consumption rate was almost constant. For the production of gluconic acid under non growth conditions, conducted in the 2 dm³ batch reactor, the effect of the pure oxygen flow rate and the biomass concentration on the gluconic acid production was investigated and an empirical equation suggested to show the dependence of the production rate r_p on the biomass concentration C_x and oxygen flow rate Q , at constant operating conditions (30°C, 300 rpm and pH 5.5).

Vunjak-Novakovic et al. (2005) showed that airlift reactors (ALRs) have great potential for industrial bioprocesses, because of the low level and homogeneous distribution of hydrodynamic shear. In this paper, they discussed the requirements for photosynthetic biomass growth in an ALR. The effects of the operating variables were analyzed using a mathematical model. They described the design and operation of this novel bioreactor and presented the first series of experimental data obtained for two different algal species in a pilot scale unit supplied with flue gases from a small power plant.

Enzymatic oxidation of glucose to gluconic acid was carried out in a 40 dm³ internal-loop airlift reactor by Markos et al. (2007 a). Due to different mixing in the

specific zones of the reactor four main sections, bottom, riser, separator and down comer, were recognized. Each zone was modelled by an adequate mixing model: bottom and separator sections by the model of ideally-stirred reactor; riser and down comer sections by the model of plug-flow reactor with axial dispersion. In the model, the effects of mass transfer, hydrodynamics, and reaction kinetics were taken into account. Here the effect of aeration was studied, also the simulation results were in good agreement with experimental data.

In the paper by Markos et al. (2007 b) mathematical modelling of the fermentation process is given for an internal loop airlift reactor (ILALR) using a tank in series model. Fermentation of gluconic acid by the strain *Aspergillus niger* was chosen as a reaction system. Fermentations were carried out in three laboratory ILARs of different scale (12, 40 and 200 dm³). Data from the smallest reactor were used for kinetic parameters estimation. All other model parameters, i.e., the gas hold-ups, the circulation velocities of the liquid and the gas, the volumetric mass transfer coefficient of oxygen were predicted by employing experimentally determined correlations from the literature. Simulated time profiles of the biomass, the substrate and the product were compared with experimental data, obtained in three laboratory ILARs, the results were in good agreement. Generally, the application of the presented model could be suitable for industrial application, particularly for process design, optimization and scale-up.

Chapter-3

MATHEMATICAL MODEL DEVELOPMENT

This chapter describes the development of mathematical model for airlift bioreactor. A mathematical model is a useful tool as it can be used for the analysis, design, control and operation of the process unit.

Mixing in airlift bioreactors is usually imperfect and mathematical models for airlift bioreactors cannot be described by either perfectly mixed (CSTR) or plug flow (PFR) reactors alone. The mixing model used in most of the previous investigations as discussed in chapter 2 dealt with airlift bioreactors as an axial dispersion model or tanks in series model.

In the present work mathematical models based on a tank-in-series with back flow and ADM are developed and simulated for a bioprocess in an airlift bioreactor under unsteady state condition.

3.1 Assumptions

Following assumptions have been made for the development of a mathematical model as used by (Znad et al., 2004).

1. Temperature and air flow rate is constant.
2. Reaction is taking place in the liquid phase only.
3. The gas hold up in the top and bottom sections are equal to the gas hold up in the riser.
4. There are no radial gradients in liquid and gas phase.
5. Saturated concentration of oxygen in liquid phase is uniform in the reactor. Change in oxygen concentration in the gaseous phase flowing through the reactor is negligible, so the material balance of oxygen in the gaseous phase can be neglected (Klein et al., 2002).
6. The back mixing in the down comer is neglected.
7. The gas hold up and mass transfer coefficient are almost constant along the riser and down comer.
8. Concentration of cell mass is used on dry basis.

9. During the multiplication process of the viable cell, no toxic compound is produced which can have adverse effect on cell growth and product formation.

3.2 Formulation of Tanks-in-Series Model

The internal airlift bioreactor is composed of a column of concentric tubes, which is divided into the region containing the gas-liquid up flow (the riser, inner tube) and the region containing the gas-liquid down flow (the down comer, the annular area). In the present work, the mixing characteristics are described by a tanks-in-series model, the flow in the airlift bioreactor is considered as flow through a series of equal sized, well mixed stirred stages or tanks and the parameter describing non ideal flow is the number of stages. Axial dispersion model is also used and described in later section.

The mixing characteristics of the riser, down comer, top and bottom sections in airlift bioreactors are different. Introducing back flow incorporates micro mixing effects into the model. The model is represented schematically in Fig. 3.1. The bottom section ($i=1$) is treated as a well mixed stage. The riser and top sections ($i=2,3, \dots, M$) are described as tanks in series with back flow. Since the flow in down comer ($j=M+1, M+2, \dots, N$) is relatively well defined, the back flow in the down comer section is neglected.

At the top section, most of gas bubbles passing upward in the riser disengage and only the rest is entrained downward by liquid re-circulation into the down comer. On the other hand, the flow in the down comer is almost single-phase and relatively well defined. Therefore, the back mixing in the down comer is neglected. The riser, including the top and bottom sections, is divided into (M) hypothetical well mixed stages. In other words, ($M - 2$) stages with back flow are used to characterize mixing in the riser. Consequently, mixing in the down comer is represented by ($N - M$) stages without back flow. The stages in the riser are numbered upwards and those in the down comer are numbered downwards.

Table 3.1 gives the numbers and distribution of stages considered in airlift bioreactor for the present study.

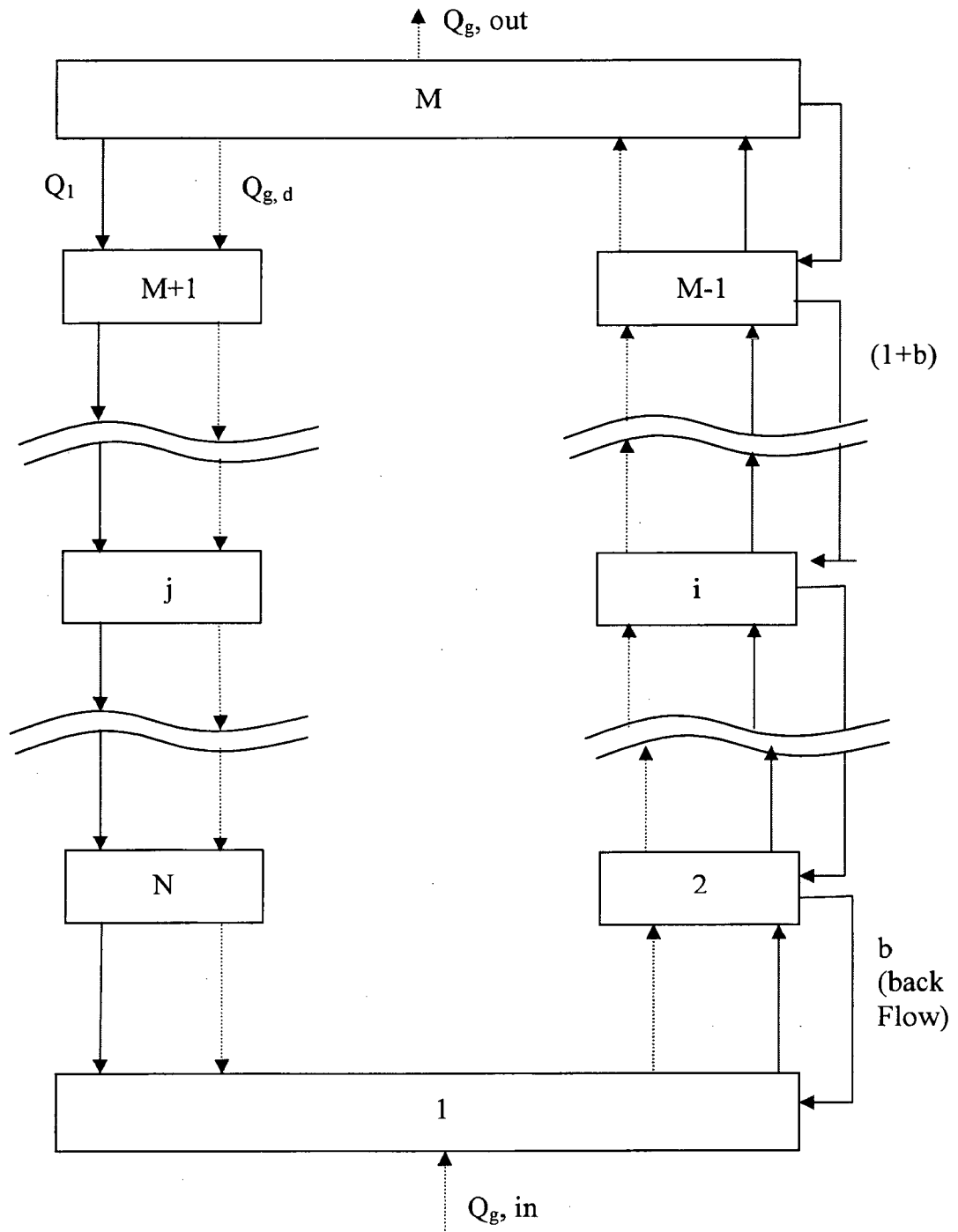


Fig 3.1 Schematic diagram of the tank-in-series model for the airlift bioreactor.

Table 3.1 Distribution of stages among sections in an ALR.

Section of ALR	Stages	Total stages
Bottom	$i=1$	1
Riser	$i=2, \dots, M-1$	2 to 21
Top	$i=M$	22
Down comer	$i=M+1, \dots, N$	23 to 44

3.3 Material Balances in Different Sections of the ALR

Material balances of the biomass (X), product (P), substrate (S) and dissolved oxygen (Co) in a hypothetical well-mixed tank or stage can be written as follows the unsteady state material balances of these components with back flow (b) provide four simultaneous first order ordinary differential equations for each stage. 'C' is referred as component either of X, P or S.

3.3.1 Bottom Section (i=1):

Bottom section is referred as section 1 and material balance diagram for it is given in Fig 3.2

Rate of change in C in section 1 = [C in by liquid flow to section 1]
 -[C out by liquid flow from section 1]
 +[C (in-out) by back flow for section 1]
 +[Rate of generation in section 1]

where C is either X, S or P

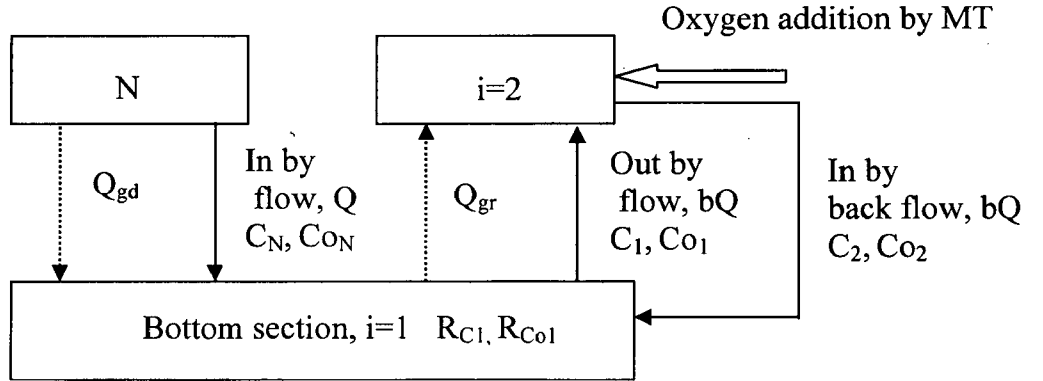


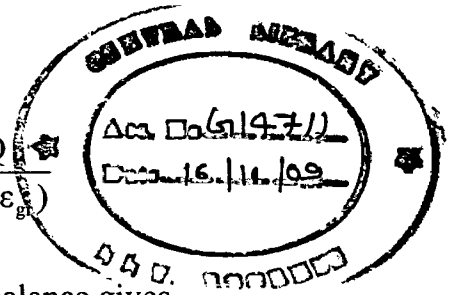
Fig 3.2 Material balances in bottom section

$$V_b(1-\epsilon_{gr}) \times \frac{dC_1}{dt} = QC_N - (1+b)QC_1 + bQC_2 + R_{C_1} \times V_b(1-\epsilon_{gr})$$

$$\frac{dC_1}{dt} = \frac{Q}{V_b(1-\epsilon_{gr})} C_N - \frac{(1+b)}{V_b(1-\epsilon_{gr})} QC_1 + \frac{bQ}{V_b(1-\epsilon_{gr})} C_2 + R_{C_1}$$

$$\frac{dC_1}{dt} = A_1 C_N - B_1 C_1 + D_1 C_2 + R_{C_1} \quad \dots (3.1)$$

$$\text{Where, } A_1 = \frac{Q}{V_b(1-\epsilon_{gr})}, B_1 = \frac{(1+b)Q}{V_b(1-\epsilon_{gr})}, D_1 = \frac{bQ}{V_b(1-\epsilon_{gr})}$$



Similarly for dissolved oxygen (Co), unsteady state material balance gives

$$\begin{aligned} \text{Rate of change in } Co \text{ in section 1} &= [\text{Co in by liquid flow to section 1}] \\ &\quad - [\text{Co out by liquid flow from section 1}] \\ &\quad + [\text{Co (in-out) by back flow for section 1}] \\ &\quad + [\text{Oxygen addition by mass transfer in section 1}] \\ &\quad + [\text{Rate of generation of oxygen in section 1}] \end{aligned}$$

Using the oxygen transfer rate per unit reactor volume to be given by

$$\text{Oxygen transfer rate} = k_L (Co^* - Co) \times \frac{A}{V}$$

and gas liquid interfacial area for unit volume as, $a = \frac{A}{V}$

$$\begin{aligned} V_b(1-\epsilon_{gr}) \frac{dCo_1}{dt} &= QCo_N - (1+b)QCo_1 + bQCo_2 \\ &\quad + (k_L a)_r (Co_1^* - Co_1) \times V_b(1-\epsilon_{gr}) + R_{Co_1} V_b(1-\epsilon_{gr}) \end{aligned}$$

$$\frac{dCo_1}{dt} = \frac{Q}{V_b(1-\epsilon_{gr})} Co_N - \frac{(1+b)Q}{V_b(1-\epsilon_{gr})} Co_1 + \frac{bQ}{V_b(1-\epsilon_{gr})} Co_2 + (k_L a)_r (Co_1^* - Co_1) + R_{Co_1}$$

$$\frac{dCo_1}{dt} = A_1 Co_N - B_1 Co_1 + D_1 Co_2 + (k_L a)_r (Co_1^* - Co_1) + R_{Co_1} \quad \dots (3.2)$$

$$\text{Where, } A_1 = \frac{Q}{V_b(1-\epsilon_{gr})}, B_1 = \frac{(1+b)Q}{V_b(1-\epsilon_{gr})}, D_1 = \frac{bQ}{V_b(1-\epsilon_{gr})}$$

3.3.2 Riser Section ($i=2, 3, \dots, M-1$):

For the micro organism, substrate and product ($C=X, S$ and P) using unsteady state material balance for the riser section shown in Fig 3.3.

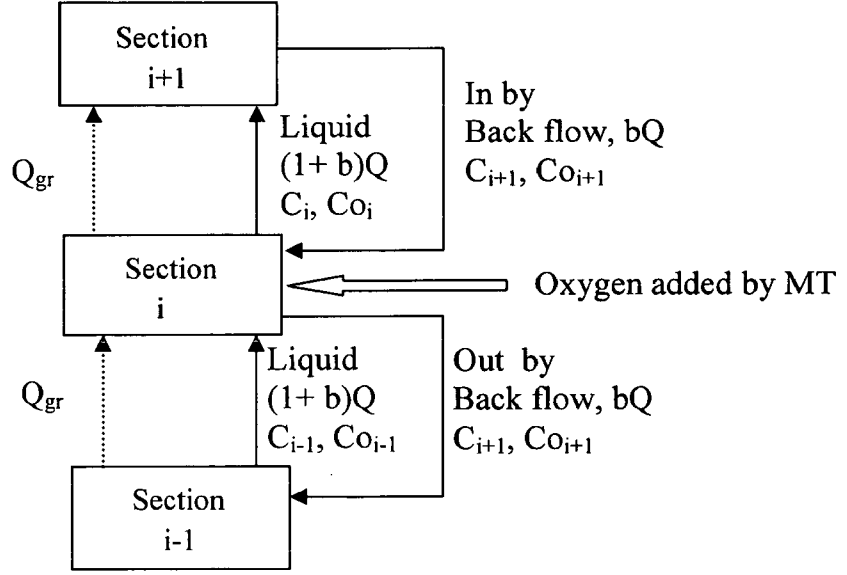


Fig 3.3 Material balances in riser section

$$\left(\frac{V_r(1-\epsilon_{gr})}{M-2} \right) \times \frac{dC_i}{dt} = (1+b)QC_{i-1} - (1+b)QC_i + bQC_{i+1} - bQC_i + R_{C_i} \times \left(\frac{V_r(1-\epsilon_{gr})}{M-2} \right)$$

$$\frac{dC_i}{dt} = \frac{(1+b)Q}{\left(\frac{V_r(1-\epsilon_{gr})}{M-2} \right)} (C_{i-1} - C_i) + \frac{bQ}{\left(\frac{V_r(1-\epsilon_{gr})}{M-2} \right)} (C_{i+1} - C_i) + R_{C_i}$$

$$\frac{dC_i}{dt} = A_2(C_{i-1} - C_i) + B_2(C_{i+1} - C_i) + R_{C_i} \quad \dots (3.3)$$

Where, $A_2 = \frac{(1+b)Q}{\left(\frac{V_r(1-\epsilon_{gr})}{M-2} \right)}$, $B_2 = \frac{bQ}{\left(\frac{V_r(1-\epsilon_{gr})}{M-2} \right)}$

Similarly, dissolved oxygen balance in section-i ($i=2,3, \dots, M-1$) can be written as

$$\left(\frac{V_r(1-\epsilon_{gr})}{M-2} \right) \times \frac{dCo_i}{dt} = (1+b)QCo_{i-1} - (1+b)QCo_i + bQCo_{i+1} - bQCo_i + (k_L a)_r (Co_i^* - Co_i) \times \left(\frac{V_r(1-\epsilon_{gr})}{M-2} \right) + R_{Co_i} \times \left(\frac{V_r(1-\epsilon_{gr})}{M-2} \right)$$

$$\frac{dCo_i}{dt} = \frac{(1+b)Q}{\left(\frac{V_r(1-\epsilon_{gr})}{M-2} \right)} (Co_{i-1} - Co_i) + \frac{bQ}{\left(\frac{V_r(1-\epsilon_{gr})}{M-2} \right)} (Co_{i+1} - Co_i) + (k_L a)_r (Co_i^* - Co_i) + R_{Co_i}$$

$$\frac{dCo_i}{dt} = A_2(Co_{i-1} - Co_i) + B_2(Co_{i+1} - Co_i) + (k_L a)_r(Co_i^* - Co_i) + R_{Co_i} \quad \dots (3.4)$$

3.3.3 Top Section (i=M):

For the micro organism, substrate and product (C=X, S and P) transient material balance over top section (Fig 3.4) gives

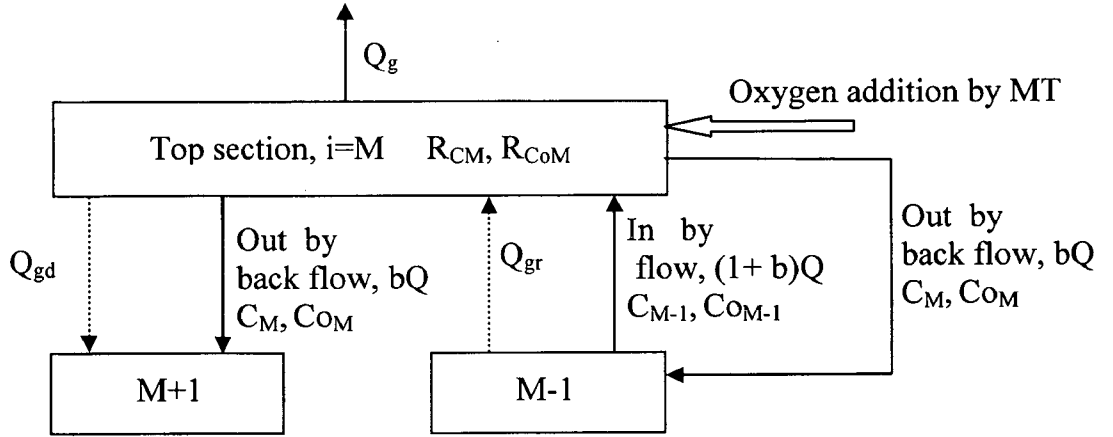


Fig 3.4 Material balances in top section

$$V_t(1-\epsilon_{gr}) \times \frac{dC_M}{dt} = (1+b)QC_{M-1} - QC_M + bQ(0-C_M) + R_{C_M} \times V_t(1-\epsilon_{gr})$$

$$\frac{dC_M}{dt} = \frac{(1+b)Q}{V_t(1-\epsilon_{gr})} (C_{M-1} - C_M) + R_{C_M}$$

$$\frac{dC_M}{dt} = A_3(C_{M-1} - C_M) + R_{C_M} \quad \dots (3.5)$$

$$\text{Where, } A_3 = \frac{(1+b)Q}{V_t(1-\epsilon_{gr})}$$

For Dissolved oxygen balance in top section-M can be written as

$$V_t(1-\epsilon_{gr}) \times \frac{dCo_M}{dt} = (1+b)QCo_{M-1} - QCo_M + bQ(0-Co_M) + (k_L a)_r(Co_M^* - Co_M) \times V_t(1-\epsilon_{gr}) + R_{Co_M} \times V_t(1-\epsilon_{gr})$$

$$\frac{dCo_M}{dt} = \frac{(1+b)Q}{V_t(1-\epsilon_{gr})} (Co_{M-1} - Co_M) + (k_L a)_r(Co_M^* - Co_M) + R_{Co_M}$$

$$\frac{dCo_M}{dt} = A_3 (Co_{M-1} - Co_M) + (k_L a)_r (Co_M^* - Co_M) + R_{Co_M} \quad \dots (3.6)$$

3.3.4 Down Comer (i=M+1, M+2, ..., N):

Similarly dynamic state material balances for down comer section (Fig 3.5) are written as

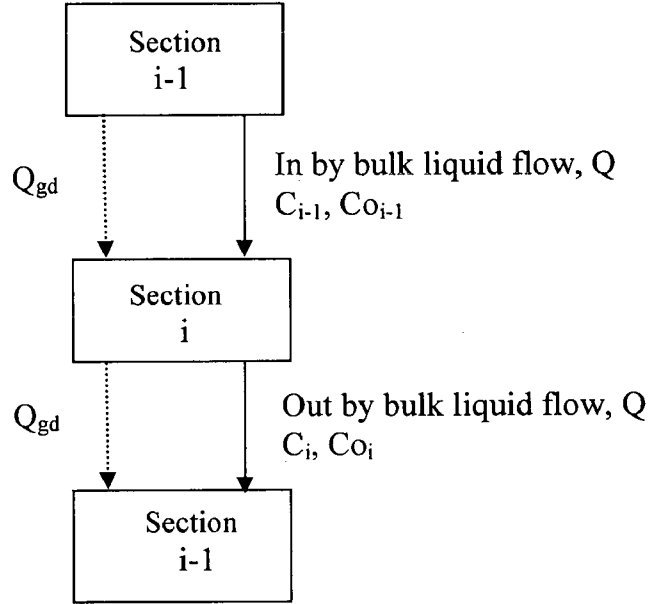


Fig 3.5 Material balances in down comer section

$$\left(\frac{V_d (1 - \epsilon_{gd})}{N - M} \right) \times \frac{dC_i}{dt} = Q C_{i-1} - Q C_i + R_{C_i} \times \left(\frac{V_d (1 - \epsilon_{gd})}{N - M} \right)$$

$$\frac{dC_i}{dt} = \frac{Q}{\left(\frac{V_d (1 - \epsilon_{gd})}{N - M} \right)} (C_{i-1} - C_i) + R_{C_i}$$

$$\frac{dC_i}{dt} = A_4 (C_{i-1} - C_i) + R_{C_i} \quad \dots (3.7)$$

$$\text{Where, } A_4 = \frac{Q}{\left(\frac{V_d (1 - \epsilon_{gd})}{N - M} \right)}, \text{ C is either X, S or P}$$

Dissolved oxygen balance in down comer section-i (i=M+1, M+2, ..., N) can be written as

$$\left(\frac{V_d (1 - \epsilon_{gd})}{N - M} \right) \times \frac{dCo_i}{dt} = Q Co_{i-1} - Q Co_i + (k_L a)_d (Co_i^* - Co_i) \times \left(\frac{V_d (1 - \epsilon_{gd})}{N - M} \right) + R_{Co_i} \times \left(\frac{V_d (1 - \epsilon_{gd})}{N - M} \right)$$

$$\frac{dCo_i}{dt} = \frac{Q}{\left(\frac{V_d(1-\epsilon_{gd})}{N-M} \right)} (Co_{i-1} - QCo_i) + (k_L a)_d (Co_i^* - Co_i) + R_{Co_i}$$

$$\frac{dCo_i}{dt} = A_4 \times (Co_{i-1} - QCo_i) + (k_L a)_d (Co_i^* - Co_i) + R_{Co_i} \quad \dots (3.8)$$

3.4 Kinetic Equations

The kinetic model presented in Znad et al. (2004 b) is used in the present study to describe the gluconic acid fermentation. In present study it is taken that the dependence of specific growth rate on carbon is assumed to follow the Logistic equation or Contois type model, which considers biomass inhibition and substrate limitation, respectively.

The biomass growth can be described as

$$R_{X_i} = \frac{dX_i}{dt} = \mu_i X_i \quad \dots (3.9)$$

The specific growth rate μ_i is defined by logistic equation and is given by

$$\mu_i = \mu_m \left(1 - \frac{X_i}{X_m} \right) \quad \dots (3.10)$$

and when given by the Contois type model it is

$$\mu_i = \mu_m \frac{S_i}{(k_{os}X_i + S_i)} \frac{Co_i}{(k_{oc}X_i + Co_i)} \quad \dots (3.11)$$

The kinetics of gluconic acid formation was based on the Luedeking-Piret equation originally developed for the fermentation of lactic acid. It is an unstructured model, which combines growth- and non growth-associated contributions towards product formation. Thus, product formation depends upon both the growth dX_i/dt and instantaneous biomass concentration X_i in a linear way

Rate of product formation,

$$\frac{dP_i}{dt} = \alpha \frac{dX_i}{dt} + \beta X_i \quad \dots (3.12)$$

Where α and β are Luedking-Piret equation parameters for growth and non growth associated product formations, respectively.

Glucose is consumed to form cell material and metabolic products as well as for the maintenance of cells. Therefore, substrate consumption can be described by the following equation

Rate of substrate uptake,

$$\frac{dS_i}{dt} = - \left[\frac{1}{Y_{x/s}} \frac{dX_i}{dt} + \frac{1}{Y_{p/s}} \frac{dP_i}{dt} \right] - m_s X_i \quad \dots (3.13)$$

Where $Y_{x/s}$ and $Y_{p/s}$ are the yield coefficients for biomass and product, respectively, and m_s is the specific maintenance coefficient.

Substituting $\frac{dP_i}{dt}$ value from eqn 3.12 yields

$$\begin{aligned} \frac{dS_i}{dt} &= - \left[\frac{1}{Y_{x/s}} \frac{dX_i}{dt} + \frac{1}{Y_{p/s}} \left(\alpha \frac{dX_i}{dt} + \beta X_i \right) \right] - m_s X_i \\ \frac{dS_i}{dt} &= - \left[\frac{1}{Y_{x/s}} + \frac{\alpha}{Y_{p/s}} \right] \frac{dX_i}{dt} - \left[\frac{\beta}{Y_{p/s}} + m_s \right] X_i \\ \frac{dS_i}{dt} &= -\gamma \frac{dX_i}{dt} - \lambda X_i \quad \dots (3.14) \end{aligned}$$

Where γ and λ are the parameters for growth and non growth associated substrate consumption, respectively and are given as

$$\gamma = \left[\frac{1}{Y_{x/s}} + \frac{\alpha}{Y_{p/s}} \right] \text{ and } \lambda = \left[\frac{\beta}{Y_{p/s}} + m_s \right]$$

The oxygen uptake rate can be described by the sum of oxygen uptake for cell growth, product formation, and cell maintenance.

$$\frac{dCo_i}{dt} = k_L a (Co_i^* - Co_i) - r_{O_i} \quad \dots (3.15)$$

$$\text{Where, } r_{O_i} = \frac{1}{Y_{X/O}} \frac{dX_i}{dt} + \frac{1}{Y_{P/O}} \frac{dP_i}{dt} + m_o X_i$$

Substituting value of r_{O_i} and $\frac{dP_i}{dt}$ into equation it gives

$$\frac{dCo_i}{dt} = k_L a (Co_i^* - Co_i) - \left[\frac{1}{Y_{X/O}} \frac{dX_i}{dt} + \frac{1}{Y_{P/O}} \left(\alpha \frac{dX_i}{dt} + \beta X_i \right) + m_o X_i \right]$$

$$\frac{dCo_i}{dt} = k_L a (Co_i^* - Co_i) - \left[\frac{1}{Y_{X/O}} + \frac{\alpha}{Y_{P/O}} \right] \frac{dX_i}{dt} - \left[\frac{\beta}{Y_{P/O}} + m_o \right] X_i$$

$$\frac{dCo_i}{dt} = k_L a (Co_i^* - Co_i) - \eta \frac{dX_i}{dt} - \psi X_i \quad \dots (3.16)$$

Where, η and ψ are the parameters for growth and non growth associated oxygen uptake, respectively and are given as

$$\eta = \left[\frac{1}{Y_{X/O}} + \frac{\alpha}{Y_{P/O}} \right] \text{ and } \psi = \left[\frac{\beta}{Y_{P/O}} + m_o \right]$$

3.5 Hydrodynamic and Mass Transfer Correlations

Airlift reactor is a reactor in which the fluid dynamics is different in each part of the reactor. The superficial gas velocity is given by

$$U_{gr} = Q_g / A_r \quad \dots (3.17)$$

The gas hold-up in the riser and the down comer are related to the overall hold up by the analytical relations.

$$\epsilon_g = \frac{A_r \epsilon_{gr} + A_d \epsilon_{gd}}{A_r + A_d} \quad \dots (3.18)$$

Empirical equation for determining the overall gas hold up can be obtained by

$$\epsilon_g = 4.334 \times 10^{-3} * \left(\frac{P_G}{V_L} \right)^{0.499} \quad \dots (3.19)$$

Another way to determine overall gas hold up is the experimental method, which can be described by the following relation.

$$\varepsilon_g = \left(\frac{h_D - h_L}{h_D} \right) \quad \dots (3.20)$$

The equation necessary for calculation of ε_{gr} or ε_{gd} is given by,

$$\varepsilon_{gd} = 0.89 \varepsilon_{gr} \quad \dots (3.21)$$

The liquid velocities in the airlift bioreactor are calculated using the well-known and widely tested model developed by Chisti et al. (2002) for airlift devices.

$$U_{Lr} = \left[\frac{2gh_D(\varepsilon_{gr} - \varepsilon_{gd})}{K_B \left(\frac{A_r}{A_d} \right)^2 \left(\frac{1}{(1 - \varepsilon_{gd})^2} \right)} \right]^{0.5} \quad \dots (3.22)$$

Where, $K_B = 11.40 \times \left(\frac{A_d}{A_b} \right)^{0.79}$

K_B is form friction loss coefficient for the bottom section.

The height of dispersion h_D is calculated from the known height of the gas-free liquid and the overall gas hold up and the relation is given as

$$h_D = \frac{h_L}{1 - \varepsilon_g}$$

The overall oxygen transfer coefficient is calculated by the following equation given by Znad et al. (2004)

$$k_L a = 1.27 \times 10^{-4} * \left(\frac{P_G}{V_L} \right)^{0.925} \quad \dots (3.23)$$

Where, $\left(\frac{P_G}{V_L} \right) = \frac{\rho_L g U_{gr}}{1 + \left(\frac{A_d}{A_r} \right)} \quad \dots (3.24)$

$(k_L a)_r$ and $(k_L a)_d$ values are selected in such a way that the following two equations are satisfied:

$$k_L a = \frac{(k_L a)_r A_r + (k_L a)_d A_d}{A_r + A_d}$$

$$(k_L a)_d = \psi (k_L a)_r \quad \dots (3.25)$$

The value of ψ is fixed at 0.8 as recommended by chisti et al (2002).

The superficial liquid velocity U_{Lr} is converted to the linear liquid velocity in the riser (V_{lr}) and the down comer (V_{ld}),

$$V_{lr} = \frac{U_{Lr}}{1 - \epsilon_{gr}} \quad \text{and} \quad V_{lr}(1 - \epsilon_{gr})A_r = V_{ld}(1 - \epsilon_{gd})A_d \quad \dots (3.26)$$

3.6 Initial Conditions

The model which have been formulated for present study is a initial value problem, thus initial values of parameters are necessary for the solution. At time $t=0$, the initial conditions are

$$X=X_0, \quad P=P_0, \quad S=S_0 \quad \text{and} \quad Co=Co_0 \quad \dots (3.27)$$

3.7 Axial Dispersion Model

The difference between the tanks in series model and axial dispersion model is that the former utilizes two parameters, the number of tanks in series N and the back flow b , while later contains only one parameter, the axial dispersion coefficient D_{ax} , which characterizes the deviations from ideal flow.

For the axial dispersion coefficient of the liquid phase towel and Ackermann gave the following equation as cited by Znad et al. (2004 a).

$$D_{ax} = 2.61 (D_r)^{1.5} (U_{gr})^{0.5} \quad \dots (3.28)$$

$$\text{Peclet number, } Pe = N / [b + 0.5] \quad \dots (3.29)$$

$$\text{Where, } Pe = (V_{lr} H_D) / D_{ax} \quad \dots (3.30)$$

V_{lr} =linear liquid velocity, m/s, H_D =height of dispersion, m

If back flow is absent, i.e., if $b=0$ then $N=Pe/2$

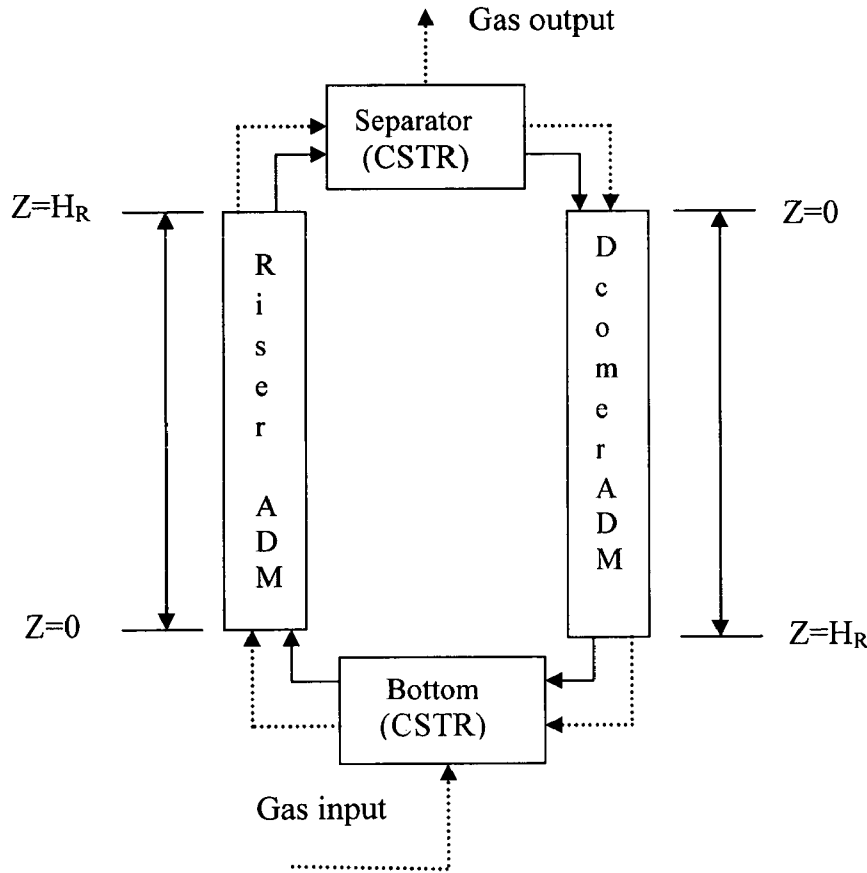


Fig 3.6 Schematic diagram of the axial dispersion model for the airlift reactor

In the present mathematical model of internal loop airlift reactor, four interconnected parts of the reactor modelled individually are involved as shown in figure 3.6.

It is expected that the bottom part and separator behave as ideally mixed compartments respectively. Modelling of non-ideal mixing in the riser and the downcomer is compared to plug flow with axial dispersion. Since the process is isothermally controlled, only the material balance is needed.

3.7.1 Bottom Section:

Material balances for oxygen ($i = O$) in bottom section of the reactor are as follows:

Gas phase material balance

$$V_B \varepsilon_{GR} \frac{dc_{i,B}^G}{dt} = (v_D^G c_{i,D}^G)_{z=H_R} - (1 - \varepsilon_{GR}) V_B k_L a_R (c_{i,B}^{*L} - c_{i,B}^L) - v_B^G c_{i,B}^G + v_{in}^G c_{i,in}^G \quad \dots (3.31)$$

Liquid phase material balance

$$V_B (1 - \varepsilon_{GR}) \frac{dc_{i,B}^L}{dt} = v_D^L c_{i,D}^L - v_B^L c_{i,B}^L + V_B (1 - \varepsilon_{GR}) r_{i,B} \quad \dots (3.32)$$

Material balances for X, S and P in bottom section of the reactor are as follows:

Liquid phase material balance for (i=X, S and P)

$$V_B (1 - \varepsilon_{GR}) \frac{dc_{i,B}^L}{dt} = v_D^L c_{i,D}^L - v_B^L c_{i,B}^L + V_B (1 - \varepsilon_{GR}) r_{i,B} \quad \dots (3.33)$$

3.7.2 Separator Section:

Material balances for oxygen (i = O) in separator section of the reactor are as follows:

Material balance on gas phase

$$V_T \varepsilon_{GR} \frac{dc_{i,T}^G}{dt} = (v_R^G c_{i,R}^G)_{z=H_R} - (1 - \varepsilon_{GR}) V_T k_L a_R (c_{i,T}^{*L} - c_{i,T}^L) - v_T^G c_{i,T}^G - v_{out}^G c_{i,out}^G \quad \dots (3.34)$$

Material balance on liquid phase

$$V_T (1 - \varepsilon_{GR}) \frac{dc_{i,T}^L}{dt} = v_R^L c_{i,R}^L + (1 - \varepsilon_{GR}) V_T k_L a_R (c_{i,T}^{*L} - c_{i,T}^L) - v_T^L c_{i,T}^L + V_T (1 - \varepsilon_{GR}) r_{i,T} \quad \dots (3.35)$$

Material balances for X, S and P in separator section of the reactor are as follows:

Material balance on liquid phase for (i=X, S and P)

$$V_T (1 - \varepsilon_{GR}) \frac{dc_{i,T}^L}{dt} = v_R^L c_{i,R}^L - v_T^L c_{i,T}^L + V_T (1 - \varepsilon_{GR}) r_{i,T} \quad \dots (3.36)$$

3.7.3 Riser / Down Comer Section:

Material balances for oxygen (i = O) in riser / down comer section of the reactor are as follows:

Gas phase on material for riser / down comer section

$$\varepsilon_{GR(D)} \frac{\partial c_i^G}{\partial t} = \varepsilon_{GR(D)} D_{aGR(D)} \frac{\partial^2 c_i^G}{\partial Z^2} - \frac{\partial (U_{GR(D)} c_i^G)}{\partial Z} - (1 - \varepsilon_{GR(D)}) k_L a_{R(D)} (c_i^{*L} - c_i^L) \quad \dots (3.37)$$

Liquid phase material balance on riser / down comer section

$$(1 - \varepsilon_{GR(D)}) \frac{\partial c_i^L}{\partial t} = (1 - \varepsilon_{GR(D)}) D_{aLR(D)} \frac{\partial^2 c_i^L}{\partial Z^2} - \frac{\partial (U_{LR(D)} c_i^L)}{\partial Z} + (1 - \varepsilon_{GR(D)}) r_i \quad \dots (3.38)$$

Material balances for X, S and P in riser / down comer section of the reactor are as follows:

Liquid phase material balance on riser / down comer section for (i=X, S and P)

$$(1 - \varepsilon_{GR(D)}) \frac{\partial c_i^L}{\partial t} = (1 - \varepsilon_{GR(D)}) D_{aLR(D)} \frac{\partial^2 c_i^L}{\partial Z^2} - \frac{\partial (U_{LR(D)} c_i^L)}{\partial Z} + (1 - \varepsilon_{GR(D)}) r_i \quad \dots (3.39)$$

For the axial dispersion model same kinetic and hydrodynamic equations as used in tanks in series model are applied. They are described in sections 3.4 and 3.5 respectively.

The model equations for ADM consists of ten ODEs in time domain and ten PDE's for riser and down comer sections in time and axial direction. For solving these equations PDEs are converted to ODEs using backward difference for partial derivatives in axial direction.

Chapter-4

SOLUTION OF THE MODEL EQUATIONS

In this chapter solution technique and its suitability has been discussed. Kinetic, design and hydrodynamic parameters are tabulated.

Model Equations and Parameters:

Model equations of different sections of airlift reactor are summarized in this section. These equations are solved using ODE solver (ode 23s) of MATLAB.

4.1 Model Equations for Solution:

4.1.1 Tanks in Series Model (Logistic Equation):

Bottom section (i=1):

$$\frac{dX_1}{dt} = A_1 X_N - B_1 X_1 + D_1 X_2 + \mu_m \left(1 - \frac{X_1}{X_m} \right) X_1$$

$$\frac{dP_1}{dt} = A_1 P_N - B_1 P_1 + D_1 P_2 + \alpha \frac{dX_1}{dt} + \beta X_1$$

$$\frac{dS_1}{dt} = A_1 S_N - B_1 S_1 + D_1 S_2 - \gamma \frac{dX_1}{dt} - \lambda X_1$$

$$\frac{dCo_1}{dt} = A_1 Co_N - B_1 Co_1 + D_1 Co_2 + (k_L a)_r (Co_i^* - Co_i) - \eta \frac{dX_i}{dt} - \psi X_i$$

Riser section (i=2,3,..., M-1):

$$\frac{dX_i}{dt} = A_2 (X_{i-1} - X_i) + B_2 (X_{i+1} - X_i) + \mu_m \left(1 - \frac{X_i}{X_m} \right) X_i$$

$$\frac{dP_i}{dt} = A_2 (P_{i-1} - P_i) + B_2 (P_{i+1} - P_i) + \alpha \frac{dX_i}{dt} + \beta X_i$$

$$\frac{dS_i}{dt} = A_2 (S_{i-1} - S_i) + B_2 (S_{i+1} - S_i) - \gamma \frac{dX_i}{dt} - \lambda X_i$$

$$\frac{dCo_i}{dt} = A_2 (Co_{i-1} - Co_i) + B_2 (Co_{i+1} - Co_i) + (k_L a)_r (Co_i^* - Co_i) - \eta \frac{dX_i}{dt} - \psi X_i$$

Top section (i=M):

$$\frac{dX_M}{dt} = A_3 (X_{M-1} - X_M) + \mu_m \left(1 - \frac{X_M}{X_m} \right) X_M$$

$$\frac{dP_M}{dt} = A_3 (P_{M-1} - P_M) + \alpha \frac{dX_i}{dt} + \beta X_i$$

$$\frac{dS_M}{dt} = A_3 (S_{M-1} - S_M) - \gamma \frac{dX_i}{dt} - \lambda X_i$$

$$\frac{dCo_M}{dt} = A_3 (Co_{M-1} - Co_M) + (k_L a)_r (Co_M^* - Co_M) - \eta \frac{dX_i}{dt} - \psi X_i$$

Down comer section (i=M+1, M+2,..., N):

$$\frac{dX_i}{dt} = A_4 (X_{i-1} - X_i) + \mu_m \left(1 - \frac{X_i}{X_m} \right) X_i$$

$$\frac{dP_i}{dt} = A_4 (P_{i-1} - P_i) + \alpha \frac{dX_i}{dt} + \beta X_i$$

$$\frac{dS_i}{dt} = A_4 (S_{i-1} - S_i) - \gamma \frac{dX_i}{dt} - \lambda X_i$$

$$\frac{dCo_i}{dt} = A_4 \times (Co_{i-1} - QCo_i) + (k_L a)_d (Co_i^* - Co_i) - \eta \frac{dX_i}{dt} - \psi X_i$$

Where, constants are defined as

$$A_1 = \frac{Q}{V_b (1 - \epsilon_{gr})}, B_1 = \frac{(1+b)Q}{V_b (1 - \epsilon_{gr})}, D_1 = \frac{bQ}{V_b (1 - \epsilon_{gr})}$$

$$A_2 = \frac{(1+b)Q}{\left(\frac{V_r (1 - \epsilon_{gr})}{M-2} \right)}, B_2 = \frac{bQ}{\left(\frac{V_r (1 - \epsilon_{gr})}{M-2} \right)},$$

$$A_3 = \frac{(1+b)Q}{V_t (1 - \epsilon_{gr})} \text{ and } A_4 = \frac{Q}{\left(\frac{V_d (1 - \epsilon_{gd})}{N-M} \right)}$$

These form a set of 4 N number of simultaneous ordinary differential equations in time. That is for N being 44, a set of 176 ODEs is to be solved. A time interval of 3 h is used for the solution.

4.1.2 Equations for Axial Dispersion Model:

Bottom section:

$$\frac{dX_{1,B}}{dt} = E_1 X_{4,D} - F_1 X_{1,B} + \mu_m \left(1 - \frac{X_{1,B}}{X_m} \right) X_{1,B}$$

$$\frac{dP_{1,B}}{dt} = E_1 P_{4,D} - F_1 P_{1,B} + \alpha \frac{dX_{1,B}}{dt} + \beta X_{1,B}$$

$$\frac{dS_{1,B}}{dt} = E_1 S_{4,D} - F_1 S_{1,B} - \gamma \frac{dX_{1,B}}{dt} - \lambda X_{1,B}$$

Riser section: (i=1, 2,..., n)

$$\frac{dX_{2,i}}{dt} = E_2 \frac{X_{2,i} - 2X_{2,i-1} + X_{2,i-2}}{(\Delta z)^2} - F_2 \frac{X_{2,i} - X_{2,i-1}}{(\Delta z)} + \mu_m \left(1 - \frac{X_{2,i}}{X_m} \right) X_{2,i}$$

$$\frac{dP_{2,i}}{dt} = E_2 \frac{P_{2,i} - 2P_{2,i-1} + P_{2,i-2}}{(\Delta z)^2} - F_2 \frac{P_{2,i} - P_{2,i-1}}{(\Delta z)} + \alpha \frac{dX_{2,i}}{dt} + \beta X_{2,i}$$

$$\frac{dS_{2,i}}{dt} = E_2 \frac{S_{2,i} - 2S_{2,i-1} + S_{2,i-2}}{(\Delta z)^2} - F_2 \frac{S_{2,i} - S_{2,i-1}}{(\Delta z)} - \gamma \frac{dX_{2,i}}{dt} - \lambda X_{2,i}$$

Top section:

$$\frac{dX_{3,T}}{dt} = E_3 X_{2,R} - F_3 X_{3,T} + \mu_m \left(1 - \frac{X_{3,T}}{X_m} \right) X_{3,T}$$

$$\frac{dP_{3,T}}{dt} = E_3 P_{2,R} - F_3 P_{3,T} + \alpha \frac{dX_{3,T}}{dt} + \beta X_{3,T}$$

$$\frac{dS_{3,T}}{dt} = E_3 S_{2,R} - F_3 S_{3,T} - \gamma \frac{dX_{3,T}}{dt} - \lambda X_{3,T}$$

Down comer section: (i=1, 2,..., n)

$$\frac{dX_{4,i}}{dt} = E_4 \frac{X_{4,i} - 2X_{4,i-1} + X_{4,i-2}}{(\Delta z)^2} - F_4 \frac{X_{4,i} - X_{4,i-1}}{(\Delta z)} + \mu_m \left(1 - \frac{X_{4,i}}{X_m} \right) X_{4,i}$$

$$\frac{dP_{4,i}}{dt} = E_4 \frac{P_{4,i} - 2P_{4,i-1} + P_{4,i-2}}{(\Delta z)^2} - F_4 \frac{P_{4,i} - P_{4,i-1}}{(\Delta z)} + \alpha \frac{dX_{4,i}}{dt} + \beta X_{4,i}$$

$$\frac{dS_{4,i}}{dt} = E_4 \frac{S_{4,i} - 2S_{4,i-1} + S_{4,i-2}}{(\Delta z)^2} - F_4 \frac{S_{4,i} - S_{4,i-1}}{(\Delta z)} - \gamma \frac{dX_{4,i}}{dt} - \lambda X_{4,i}$$

Where, $E_1 = \frac{v_D^L}{V_B(1-\epsilon_{GR})}$, $F_1 = \frac{v_B^L}{V_B(1-\epsilon_{GR})}$

$$E_2 = D_{aLR}, F_2 = \frac{1}{(1-\epsilon_{GR})}$$

$$E_3 = \frac{v_R^L}{V_T(1-\epsilon_{GR})}, F_3 = \frac{v_T^L}{V_T(1-\epsilon_{GR})}$$

$$E_4 = D_{aLD}, F_4 = \frac{1}{(1-\epsilon_{GD})}$$

4.2 Kinetic Parameters:

Kinetic parameters of contoio model are taken from the work of Znad et al. (2004) and are tabulated in Table 4.1.

Table 4.1 Kinetic parameters of contoio model

Sl. No.	Parameter	Values
1.	μ_m	0.3610
2.	α	4.5865
3.	β	1.3757
4.	γ	3.9868
5.	λ	0.9660
6.	η	1.52
7.	ψ	0.0808
8.	kos	21.239
9.	koc	0.004134

Kinetic parameters of logistic equation are given in table 4.2. For the determination of maximum specific growth rate and initial cell mass concentration, experimental data and value of maximum cell mass concentration, as used by Jian-Zhong et al (2003)

Table 4.2 Kinetic parameters of logistic equation.

Sl. No.	Parameter	Values
1.	μ_m	0.1335
2.	X_0	0.308
3.	α	18.028
4.	β	0.751
5.	γ	13.144
6.	λ	0.604
7.	η	0.58
8.	ψ	0.9339

4.3 Estimated Design and Hydrodynamic Parameters:

Following parameters have been calculated from the hydrodynamic and mass transfer correlations given in last chapter, for the present airlift bioreactor and used in the simulation.

Table 4.3 Estimated design and hydrodynamic parameters:

Sl. No.	parameter	units	Value
1.	Working volume (V)	dm^3	4.5
2.	$k_L a$	h^{-1}	94.7312
3.	P_g/V	W/m^3	319.30229
4.	ϵ_g	-	0.077
5.	Q_g	m^3/s	1.3×10^{-4}
6.	Q	m^3/s	3.6×10^{-4}
7.	U_{gr}	m/s	0.10143
8.	U_{lr}	m/s	0.2633
9.	h_D	m	1.1159
10.	Pe	-	44.76
11.	N	-	44
12.	M	-	22

4.4 Solution Scheme Adopted

In order to predict the performance of the model, solution of model equations is very essential. The system of partial differential equations in axial dispersion model is converted to a set of ordinary differential equations using the backward finite difference method for the space coordinate. So, the developed mathematical model in this chapter consists of a set of first order ordinary coupled differential equations. These equations constitute initial value problem (IVP), which has been solved using ODE solvers (ode 23s), a routine for stiff differential equations of MATLAB.

Chapter-5

RESULTS AND DISCUSSION

Mathematical models for the production of gluconic acid from glucose in an airlift reactor are developed in chapter 3. The mathematical models use logistic equation and Contois equation to represent concentrations of biomass, gluconic acid, glucose and dissolved oxygen in the reactor. The airlift bioreactor is divided into four sections, namely bottom, riser, top and down comer sections. The reactor has been modelled by two approaches i.e. tanks-in-series model and axial dispersion model. In tanks in series model total reactor is divided into 44 well mixed stages, where as in axial dispersion model bottom and separator sections are considered as CSTRs, riser and down comer sections are represented by axial dispersion model. The model uses four coupled ordinary differential equations to represent concentration of four variables, namely biomass, product, substrate and DO in each hypothetical well mixed stage of the reactor. Similarly, ADM for riser and down comer is described by 5 partial differential equations for each section. The complete set of model equations for tanks-in-series model is given in section 4.1.1 of chapter 4. The set of kinetic and hydrodynamic parameters are given in table 4.1, 4.2 and 4.3 respectively in chapter 4. Axial dispersion model is described in section 4.1.2 of chapter 4. The reaction mechanism is provided in chapter 2.

The model has been validated by comparing simulation run results with the experimental data of Znad et al. (2004). In the present chapter the validated model is then used to predict the variation of output parameters with input parameters. Variation of initial cell biomass concentration (X_0) and air flow rate as shown in Table 5.1 is used to predict the fermentation behaviour in an airlift bioreactor. Dissolved oxygen profile along the axial direction in airlift bioreactor has been studied. Axial dispersion model and tanks in series are compared for biomass, product and substrate concentration profiles.

Table 5.1 Variation range of parameter for simulation.

Sl. No.	Parameter	Range of parameter	Model used
1.	Initial biomass concentration	$0.308 \pm 0.2032 \text{ g/dm}^3$	Logistic equation
2.	Air flow rate	5 - 25 dm^3/min	Contois model

5.1 Analysis of Experimental Data

The experimental data for concentrations of biomass, product, substrate and dissolved as given in Appendix B.1 has been taken from Znad et al. (2004). The above mentioned parameters have been plotted as a function of time for a batch operation period of 51 h. The profiles are shown in figures 5.1 through 5.4, respectively to develop in depth understanding of the process.

5.1.1 Variation of Biomass Concentration with Time

Figure 5.1 shows the variation of biomass concentration (X) with batch time available for the growth of microorganisms in the gluconic acid fermentation by *Aspergillus niger* at the constant operating conditions (30⁰ C and 6.0 pH). From the plot, following facts are observed.

- After seeding a liquid medium with an inoculum of living cells into the reactor, only air is added to the culture for its growth. Four different phases of the growth cycle are observed. These are (i) lag phase, (ii) exponential phase, (iii) deceleration phase and (iv) stationary phase.
- The first phase is lag phase, which varies up to 6 h period. In this phase practically there is no apparent growth of biomass, which indicate that the cells are in process of adapting to the environmental conditions and that new growth will eventually begin.
- In the exponential phase, which is observed from 6 to 25 h period, microbial cell growth proceeds at the maximum possible rate. During this period, nutrients are sufficient. This provides an ideal environment condition for the growth of microorganisms. The strain start to form gluconic acid and therefore cell growth and gluconic acid production take place simultaneously. However, in batch fermentations exponential growth is of limited duration and as nutrient conditions change, growth rate decreases.
- The third phase is deceleration phase, which ranges from 25 to 42 h. Limited nutrients and changing environmental conditions in the system leads to deceleration of the growth of cells.

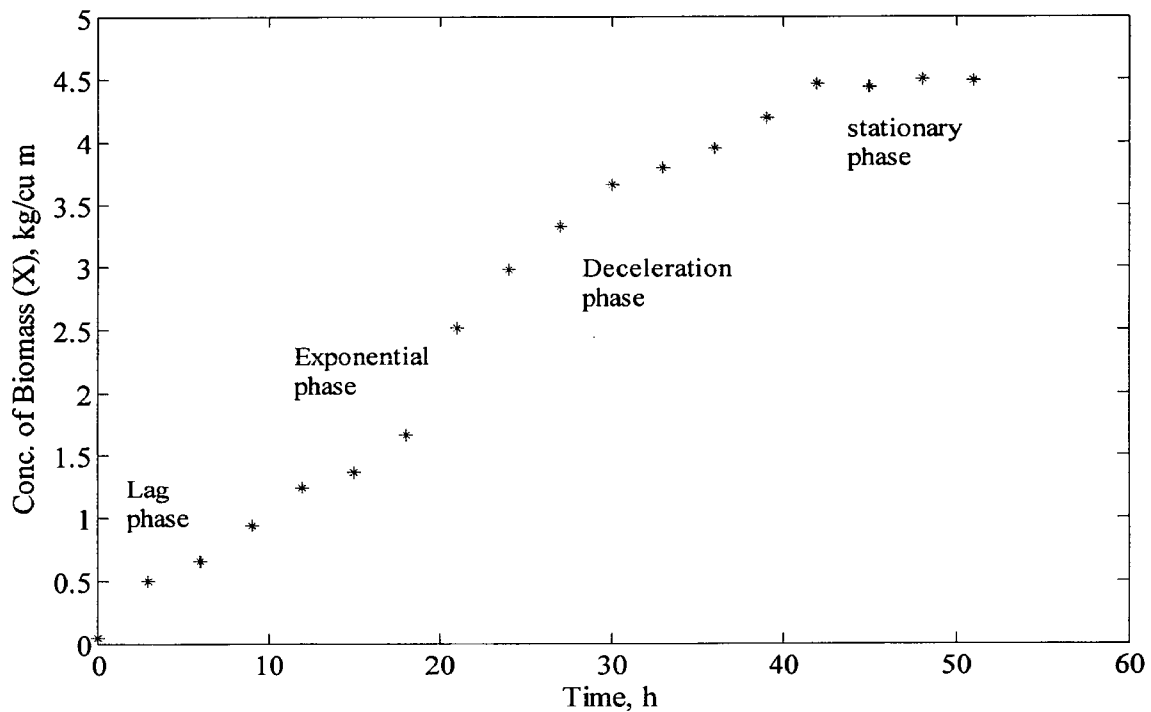


Fig 5.1 Concentration of biomass as a function of time

- In the fourth phase, seen from 42 h to 51 h period the cell mass growth becomes stable and in this time the cell production and cell death rate becomes equal. Once the limiting substrate become scarce, the overall growth can no longer be obtained because of nutrient exhaustion resulting into the death phase.

5.1.2 Variation of Gluconic Acid (GA) Concentration with Time

Figure 5.2 is plotted to show the variation of gluconic acid concentration with batch time at constant operating conditions. From this figure, following facts are observed.

- Once the cell start growing, the microorganisms start to hydrolyze gluconolactone to form gluconic acid and hence concentration of GA increases linearly with batch time.
- The hydrogen peroxide produced during the process is decomposed to provide oxygen, which is again utilized during the process. As shown in the figure, initially the gluconic acid formation is very little up to a period of about 6 h, but as soon as the cells grow, the product is formed at a constant rate after 10 h indicated by the constant slope of the plot.

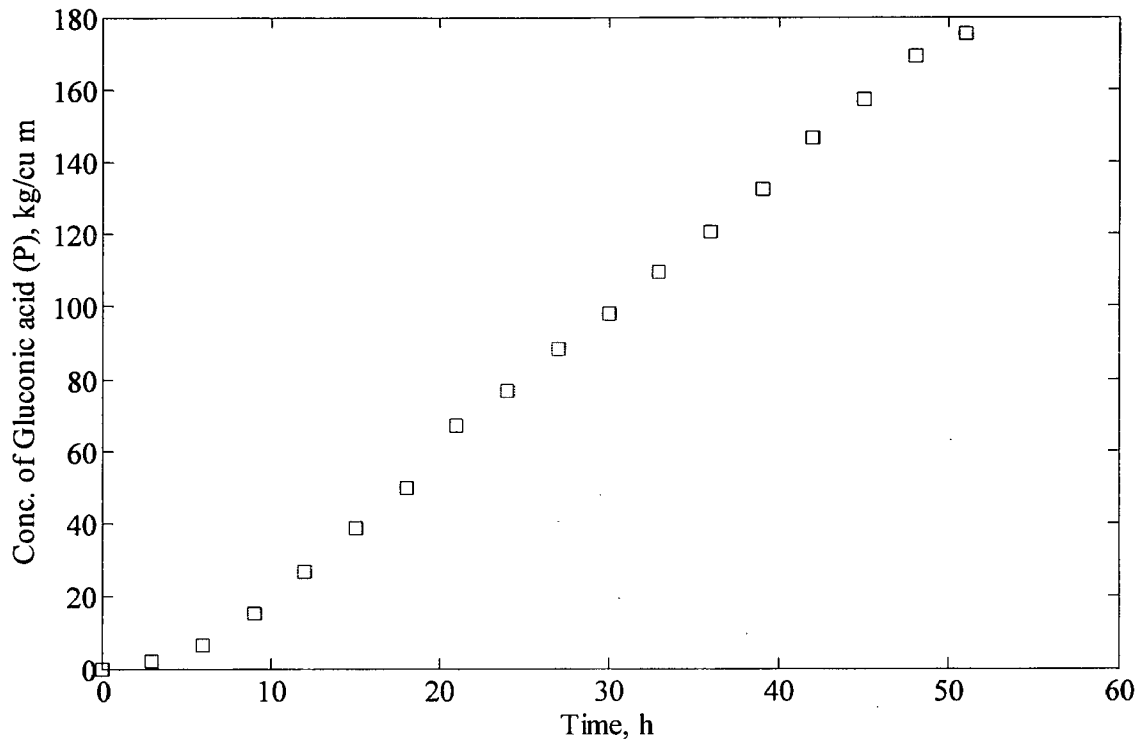


Fig 5.2 Concentration of gluconic acid as a function of time

5.1.3 Variation of Glucose Concentration with Time

Figure 5.3 is plotted to show the variation of glucose concentration with time. From the figure, following facts are evident.

- Growth of microorganisms starts as soon as they adapted themselves to the environmental conditions. Initially in the lag phase, they utilize the glucose slowly, which increase rapidly in the exponential phase as shown in the figure 6.3.
- The rate of glucose consumption is less in the first 10 h. However, the consumption rate is maintained after 10 h. This may be attributed to the constant rate of GA production as can be seen from the figure 6.2.
- Glucose consumption result in the formation of biomass and subsequently to the formation of GA.

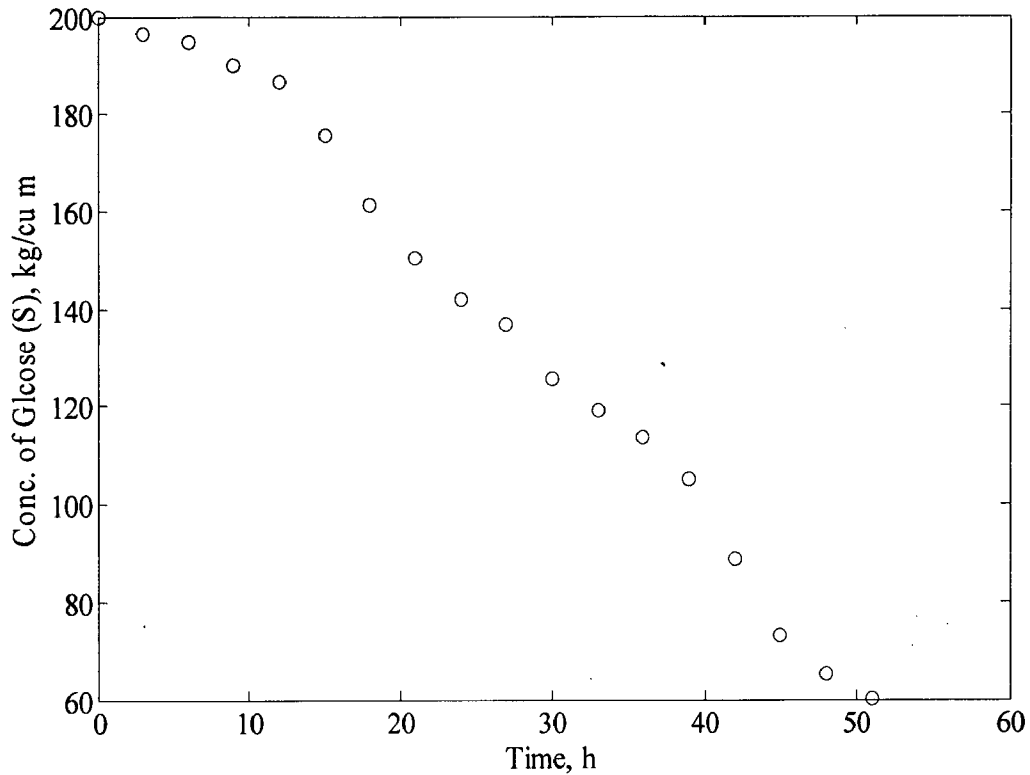


Fig 5.3 Concentration of glucose as a function of time

5.1.4 Variation of Dissolved Oxygen Concentration with Time

Figure 5.4 is a plot of dissolved oxygen concentration with time. From the figure, following facts are observed.

- Saturated DO concentration at air supply rate of $7.8 \text{ dm}^3/\text{min}$ is 0.00651 kg/m^3 in an ALBR. This value rapidly reduces to 0.0028 kg/m^3 in the first 15 h duration of batch time. During this period, the oxygen requirement is maximum because in this period oxygen supply takes place by dissolved oxygen only.
- Beyond 15 h of duration, the H_2O_2 decomposition become prominent and so then the concentration of DO fall slowly to 0.0018 kg/m^3 at 42 h.

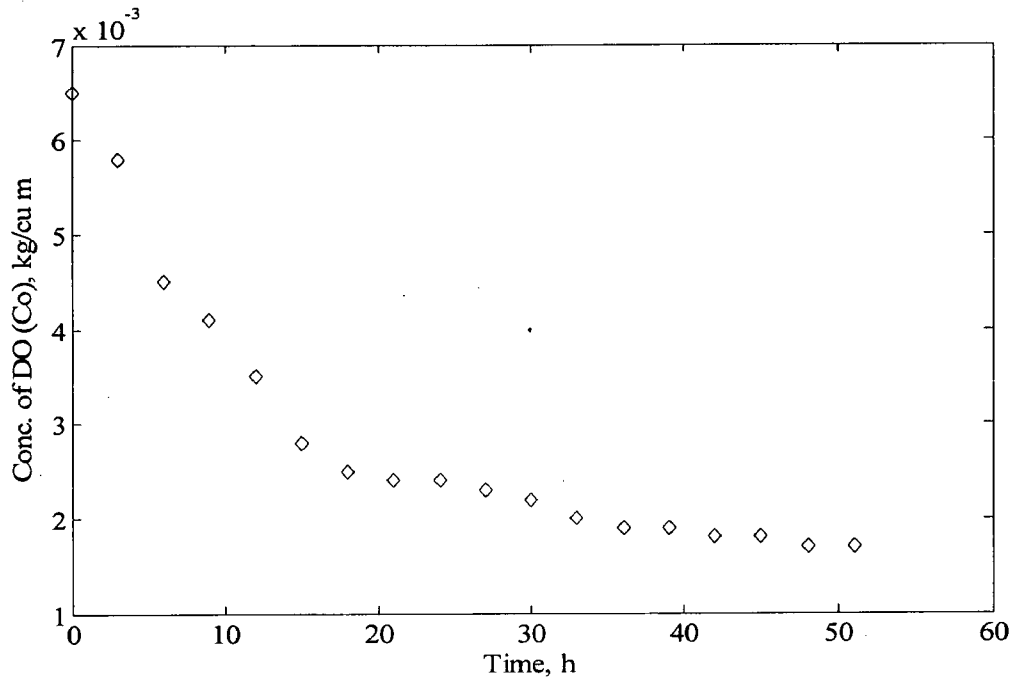


Fig 5.4 Concentration of dissolved oxygen as a function of time

5.2 Validation of Models

The model has been validated by comparing simulation results with experimental data given in Appendix B.1. Logistic equation and contoits model are tested to represent the concentration profiles of biomass, gluconic acid, substrate and dissolved oxygen with batch time as shown in figures 5.5 and 5.6.

5.2.1 Experimental and Predicted Biomass Concentration

Figure 5.5 and 5.6 shows the comparison between model simulation results and experimental data (Znad et al., 2004) for biomass concentration in an ALBR. From the figure, following facts can be observed.

- Prediction of biomass concentration by logistic equation is very good except for the first 3 h of batch time (lag phase) as shown in figure 6.5. During this period predicted value is 0.308 g/l where as the experimental value is 0.04 g/l. This discrepancy has also been observed by Jian-Zhong et al. (2003). Similarly simulation over predicts biomass concentration for some period in exponential phase.
- The contoits model under predicts the biomass concentration up to first 15 h. However, the prediction is good for in the batch period from 15 h to 42 h. Further, it over predicts beyond 42 h as shown in figure 6.6.

- Thus, for the prediction of biomass concentration, the logistic equation is more preferable in the ALBR.

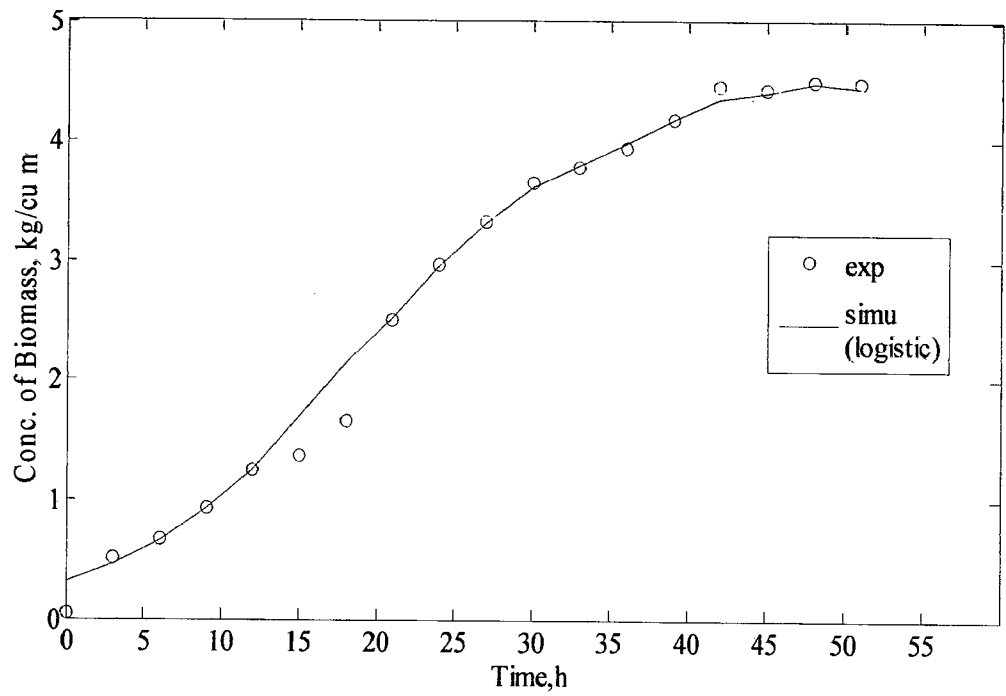


Fig 5.5 Cell biomass concentration profile represented by logistic equation

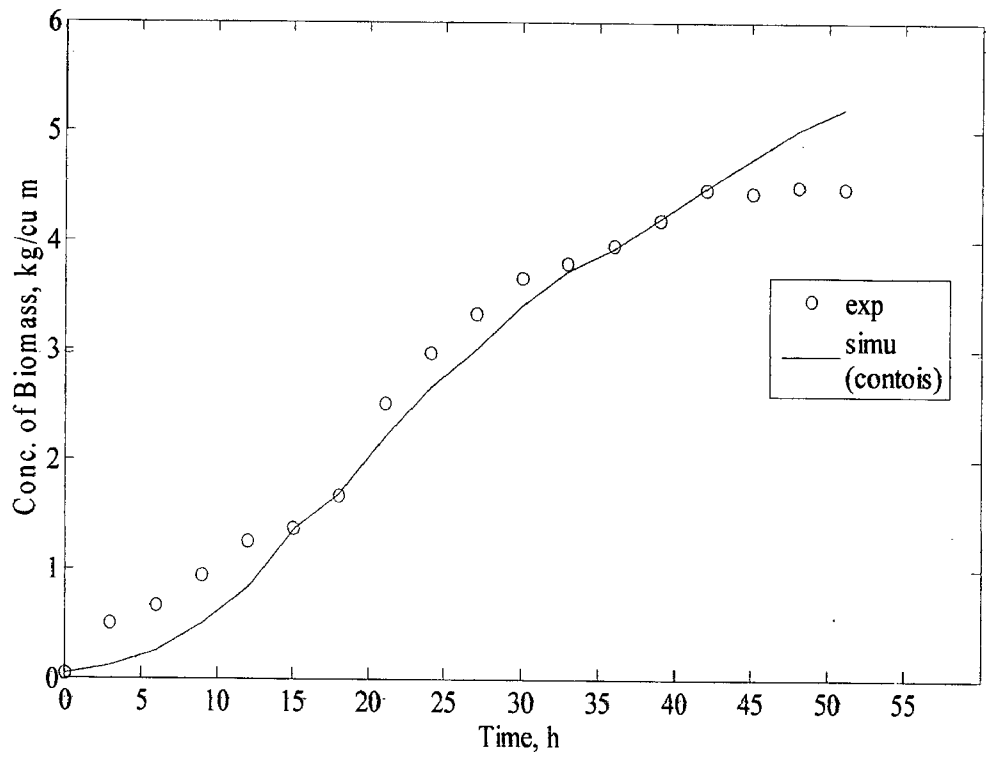


Fig 5.6 Cell biomass concentration profile represented by contois equation

5.2.2 Experimental and Predicted Gluconic Acid Concentration

Figure 5.7 and 5.8 shows the comparison of model predictions with experimental data for gluconic acid concentration in an ALBR. From the figure, following facts can be observed.

- Figure 5.7 shows that the representation of gluconic acid concentration by logistic equation in an ALBR is very good throughout the batch period.
- Contois model is not in agreement with the experimental data in the exponential as well as in the stationary phase.
- Thus, for the prediction of the gluconic acid concentration in an ALBR, the logistic equation is more accurate.

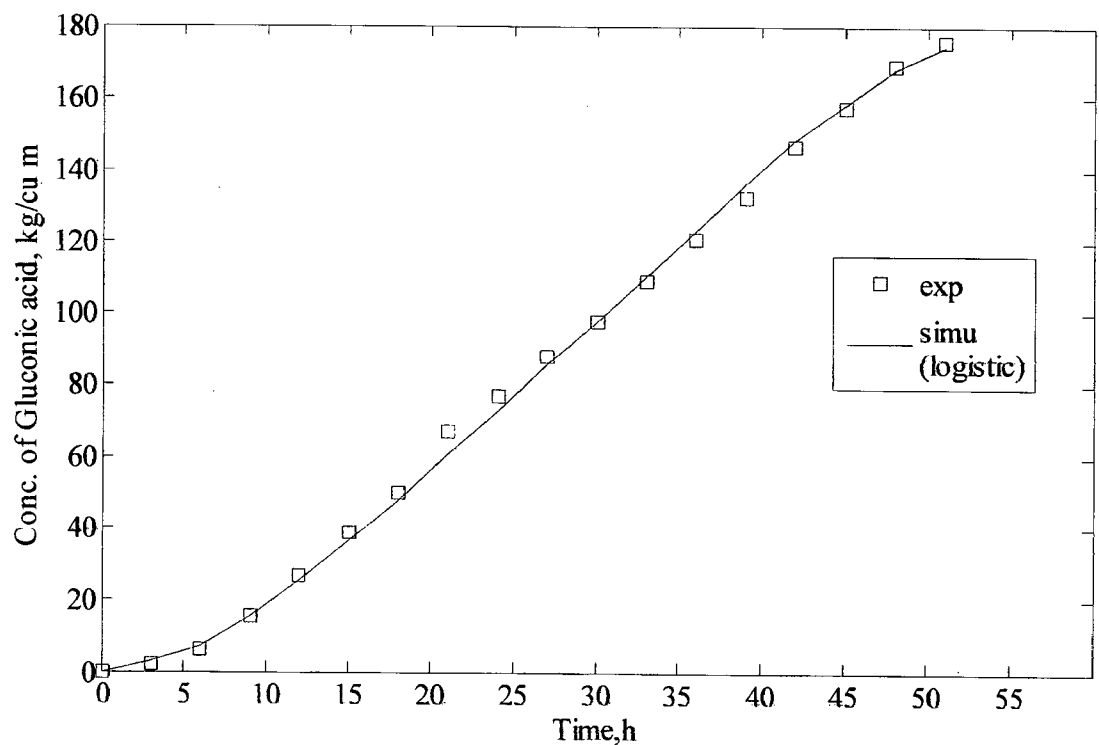


Figure 5.7 Gluconic acid concentration profile represented by logistic equation

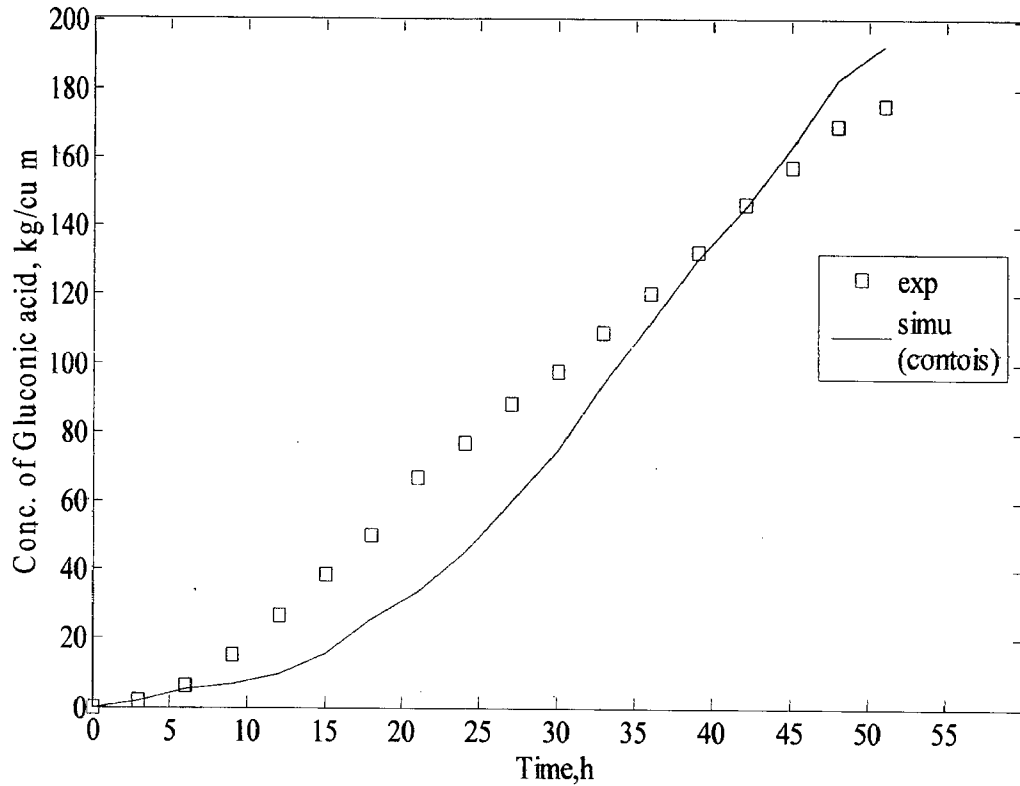


Figure 5.8 Gluconic acid concentration profile represented by contoiois equation

5.2.3 Experimental and Predicted Glucose Concentration

Figure 5.9 and 5.10 shows the comparison of model predictions with experimental data for gluconic acid concentration in an ALBR. From the figure, following facts can be observed.

- Figure 5.9 shows that the representation of glucose concentration in an ALBR can be accurately predicted by the logistic equation.
- Contois model over predicts the glucose concentration in an ALBR in the period from 3 h to 39 h as shown in the figure.
- Thus, the prediction of glucose concentration in an ALBR is better by logistic equation as compared to that of contoiois model.

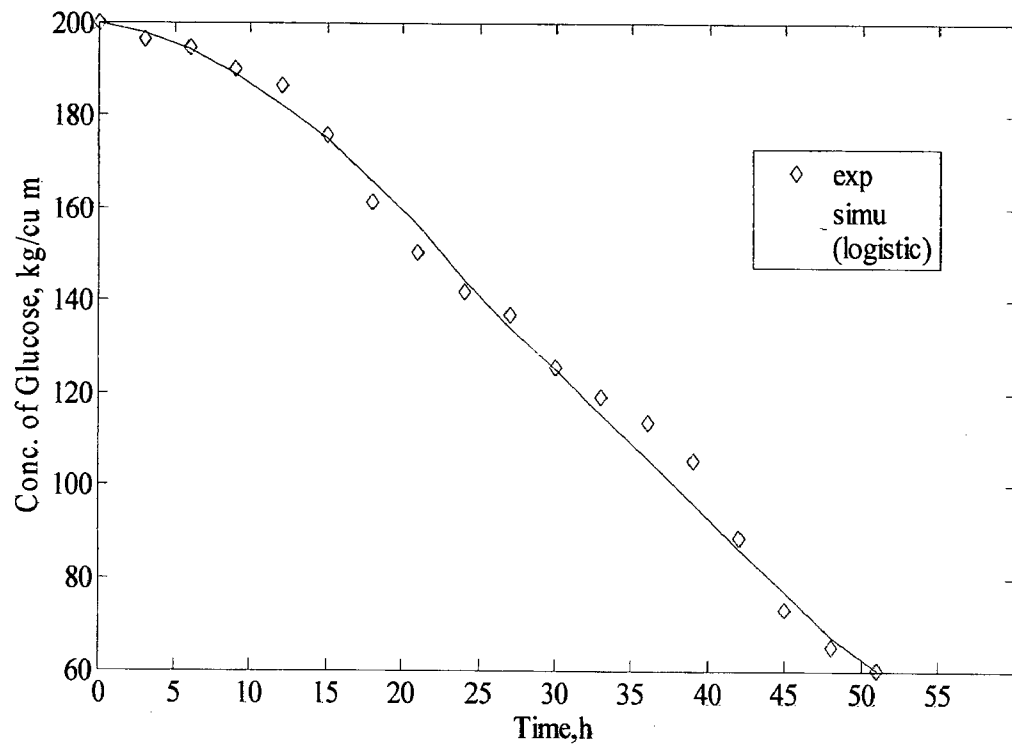


Figure 5.9 Glucose concentration profile represented by logistic equation

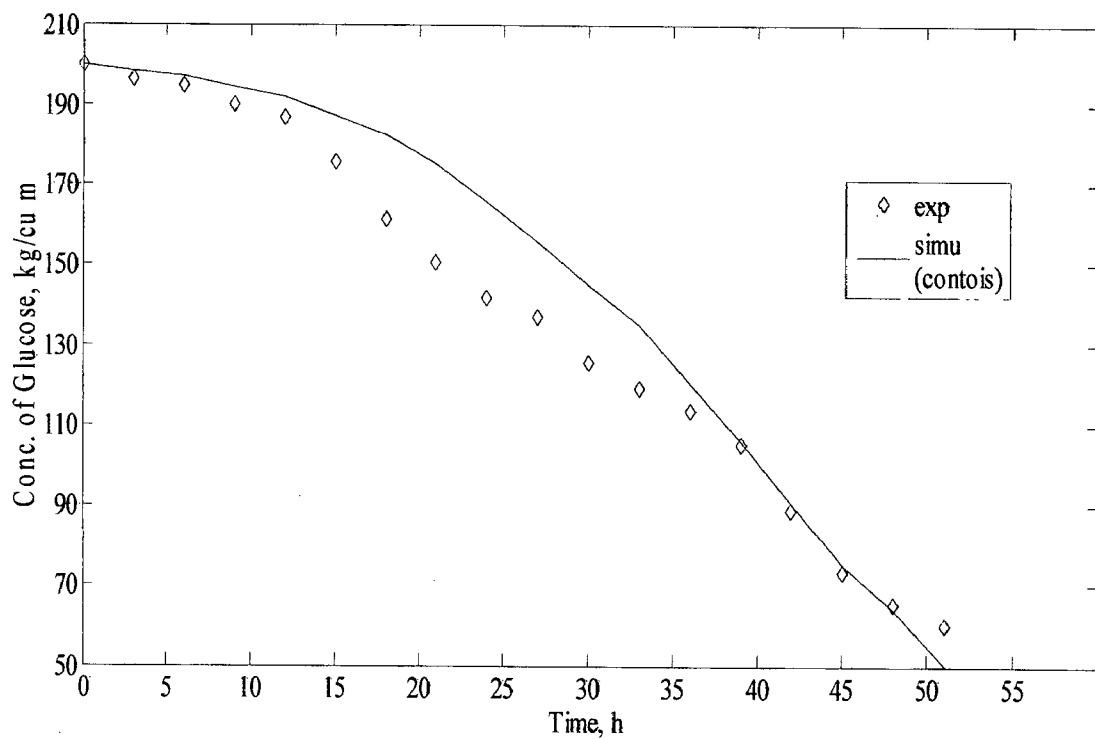


Figure 5.10 Glucose concentration profile represented by conto is equation

5.2.3 Experimental and Predicted DO Concentration

Figure 5.11 and 5.12 show the comparison of model predictions with experimental data for dissolved oxygen concentration in an ALBR. From these figures, observations are made.

- Figure 5.11 shows that logistic equation fails to represent the DO concentration in the ALBR. The large deviation in predicted values from actual values is observed. The reason for such behaviour is that the model equations do not take into account DO concentration.
- The prediction by contoits model (Fig 5.12) is in good agreement since it accounts for the DO concentration through the entire range of batch time. This behaviour indicates that the contoits model is better for the study of DO concentration within the ALBR.

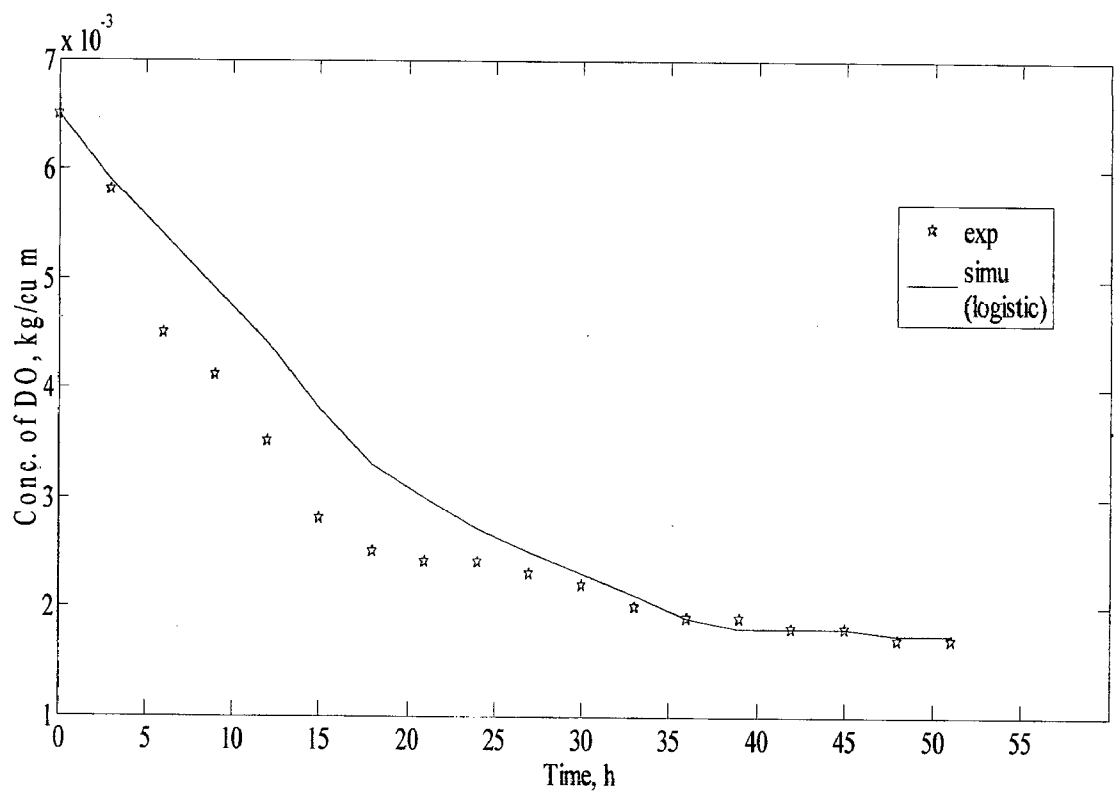


Figure 5.11 Dissolved oxygen concentration profile represented by logistic equation

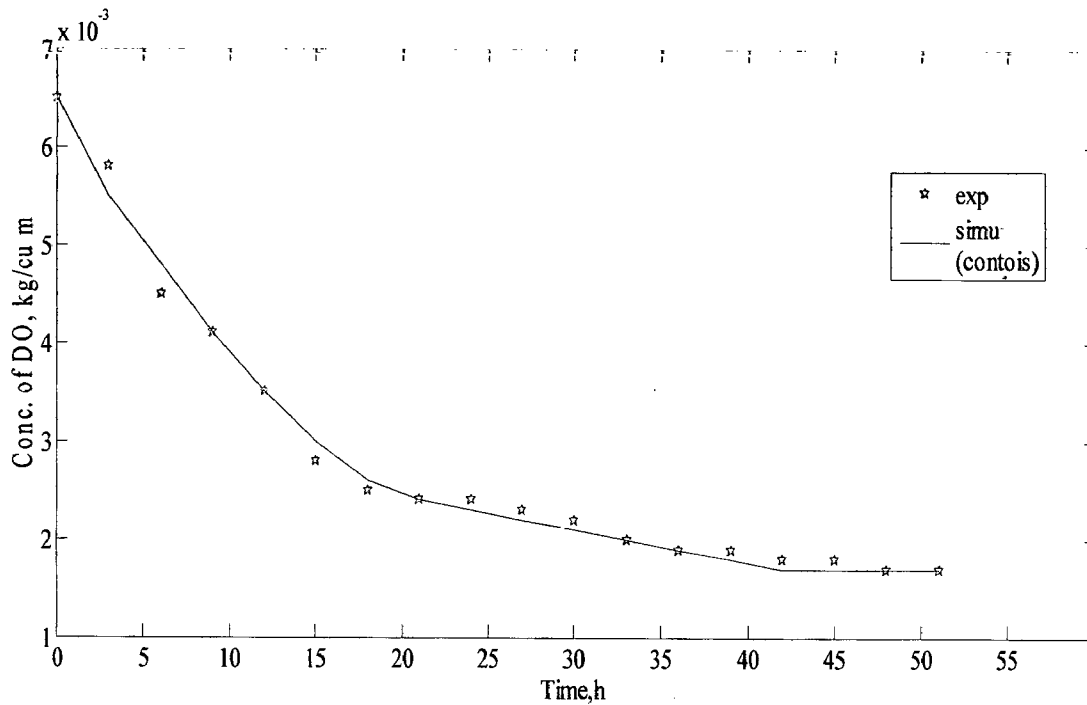


Figure 5.12 Dissolved oxygen concentration profile represented by Contois equation

5.3 Effect of Variation of Parameters based on Model Predictions:

It had been observed that initial cell mass, airflowrate (gas hold up) significantly influence the fermentation in an airlift reactor. The effect of variation of operating parameters as given in Table 5.1 studied to predict the behaviour of the biological process in an ALBR. Logistic equation is used to predict the effect of variation in time dependent biomass, gluconic acid and glucose concentrations.

5.3.1 Effect of Initial Cell Mass Concentration (X_0)

Different initial biomass values using logistic equation are tested and simulated results are shown in figure 5.13 through 5.15.

- Higher initial cell concentration results in rapid growth of biomass, and subsequently immediate formation of product and reduces the batch time considerably as steady state values are obtained in shorter period.

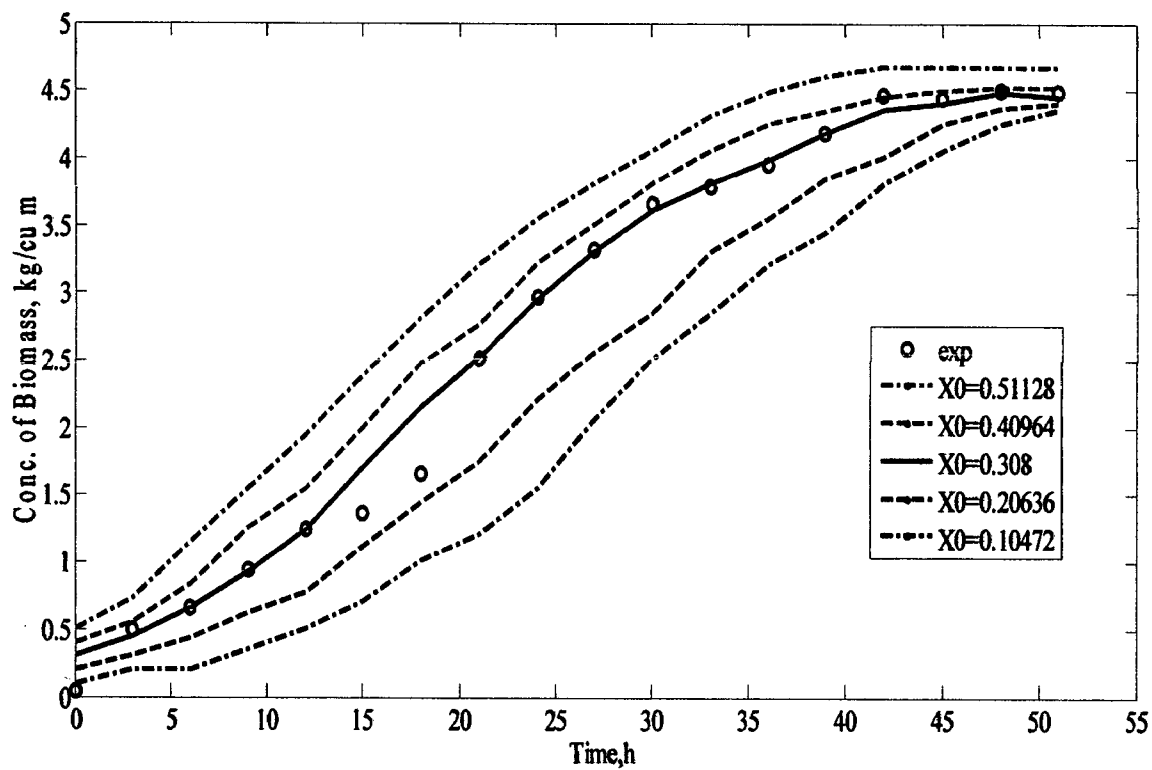


Figure 5.13 Effect of change in initial cell mass on biomass growth by logistic equation

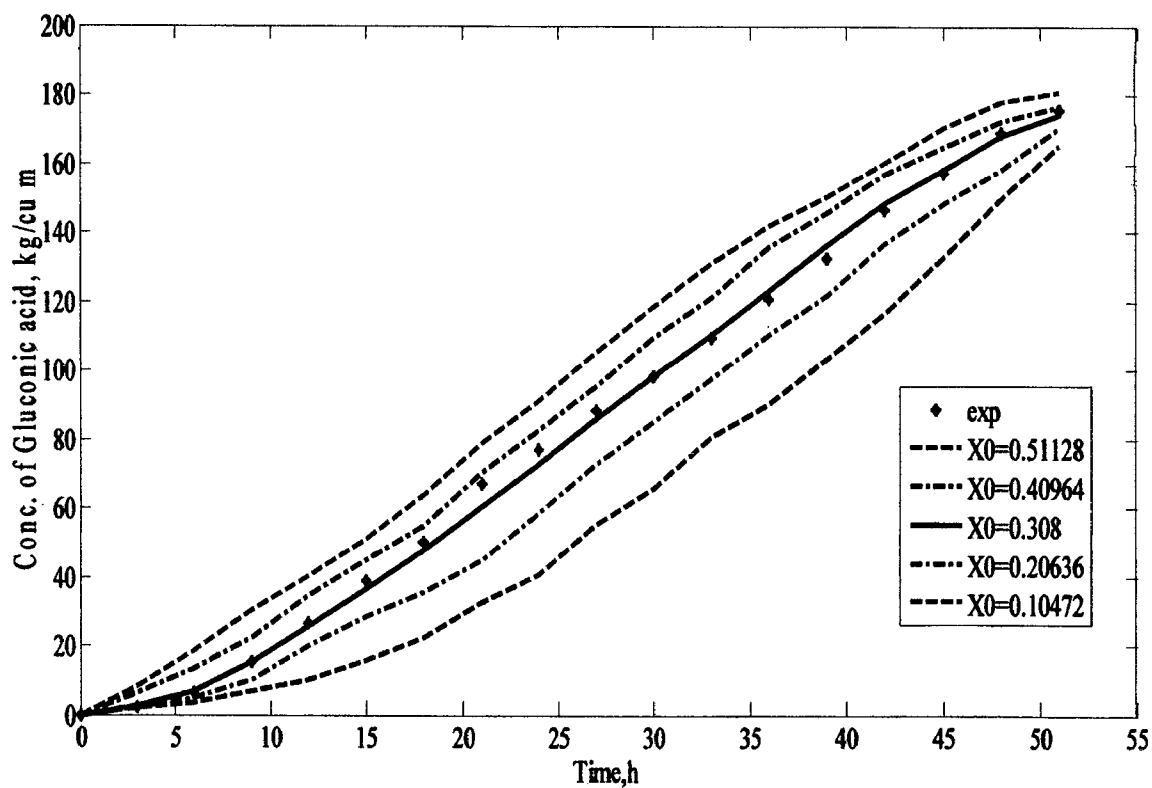


Figure 5.14 Effect of change in initial biomass concentration on gluconic acid production by logistic equation

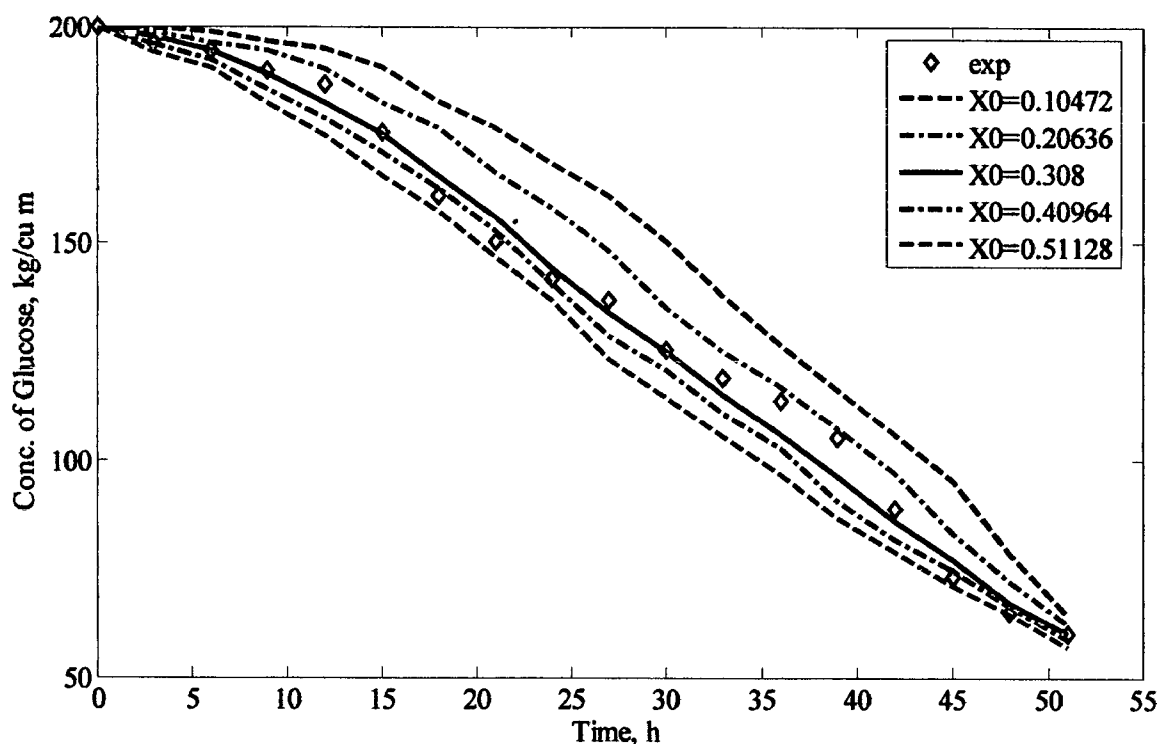


Figure 5.15 Effect of change in initial biomass concentration on glucose consumption by logistic equation

- As seen from figure 5.14, the gluconic acid formation of 163 g/dm^3 is achieved in 42 h instead of 51 h if the X_0 is increased from 0.10472 g/dm^3 to 0.5112 g/dm^3 .
- The glucose concentration falls rapidly when higher initial cell mass concentration is used as can be seen from figure 5.15. These profiles indicate that the higher cell mass reduces the batch time for the same yield of gluconic acid.

5.3.2 Effect of Airflow Rate (Q_g)

Contois model is used to study the effect of airflow rates. Figures 5.16, 5.17 and 5.18 show the effect of airflow rate on the biomass growth, GA and substrate concentrations, keeping 57 h as a fixed time for the duration of fermentation. The biomass growth increased with increase in airflow rate in the range of 5 to $25 \text{ dm}^3/\text{min}$. The production of biomass and GA increased with the increase in aeration rate and stabilize at an airflow rate of $20 \text{ dm}^3/\text{min}$. Beyond $20 \text{ dm}^3/\text{min}$ the effect of airflow rate on the biomass growth and GA produced is not significant. This can be attributed to the fact that high airflow rates can lead to high gas hold ups, enhanced bulk mixing and improved DO and mass transfer, which promotes the biomass growth and consequently the gluconic acid.

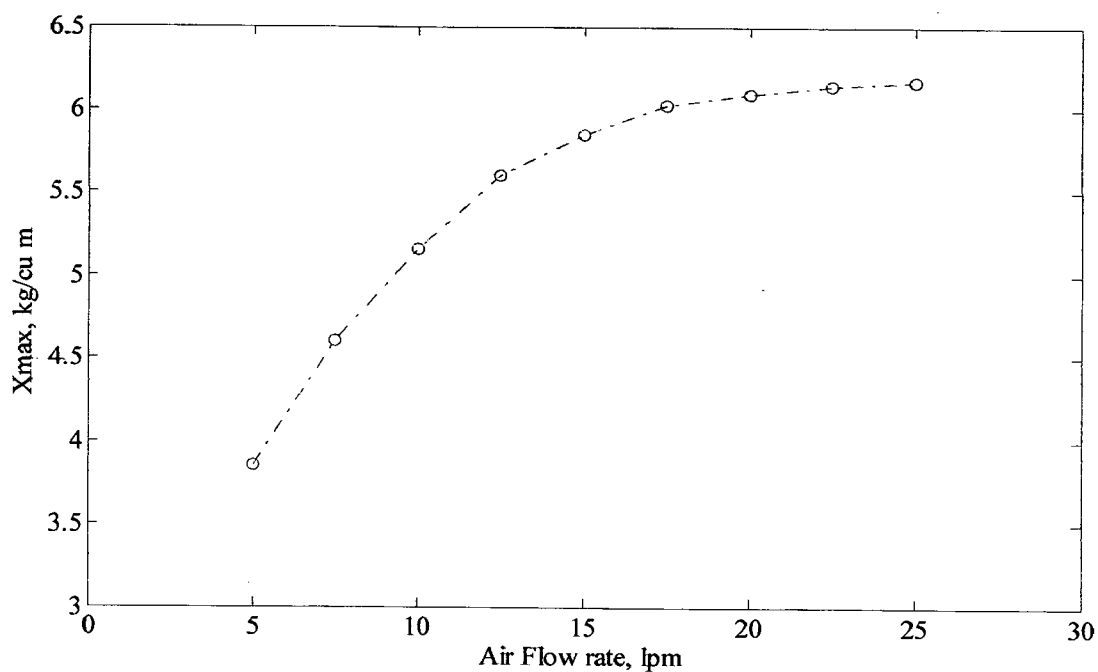


Figure 5.16 Effect of airflow rate on the biomass concentration at 57 h of fermentation

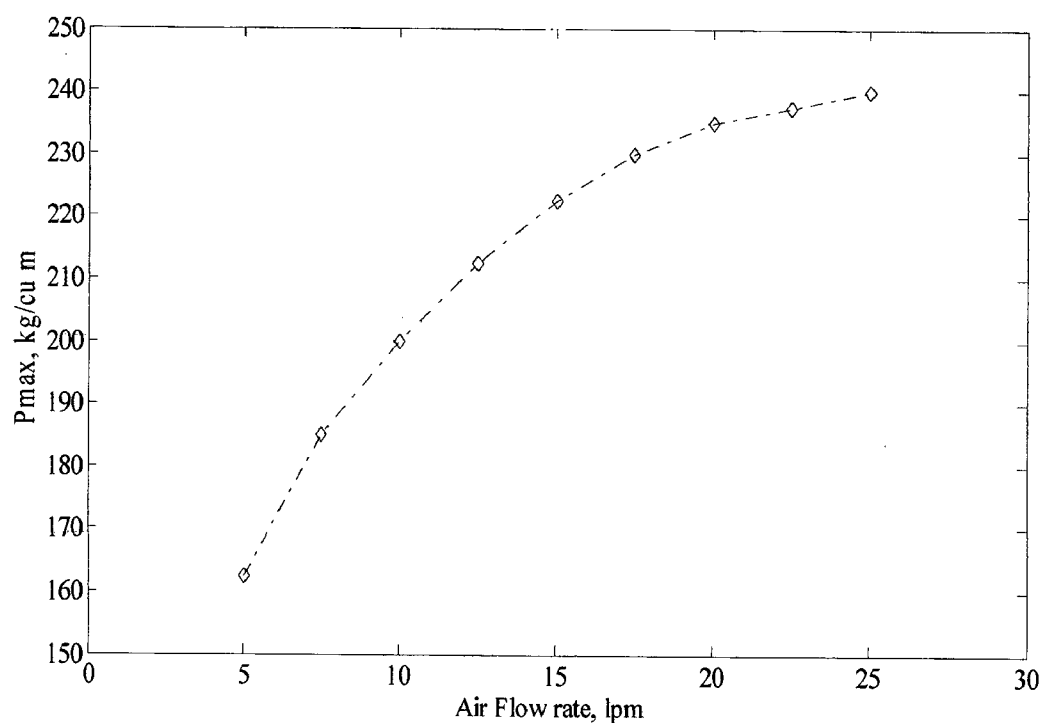


Figure 5.17 Effect of airflow rate on the gluconic acid at 57 h of fermentation

When the airflow rate exceeds $20 \text{ dm}^3/\text{min}$, the increase in the biomass growth with airflow rate is reduced. The reason of this is that because high airflow rate produced a high

shear stress, which could potentially lead to cellular damage, consequently reducing the ability of cells to produce gluconic acid. Another reason could be, that higher airflow rates resulted in higher respiration rates, potentially leading to a significant decrease in glucose source (substrate) availability for any purpose, including gluconic acid synthesis as shown in Figure 5.18. The results show that there was an optimum range of airflow rate from 5 to 20 dm^3/min for gluconic acid fermentation in a 4.5 dm^3 internal loop airlift bioreactor. This leads to an additional process benefit of minimizing the costs of compressed air, a major contributor to the cost of running a large-scale airlift bioreactor.

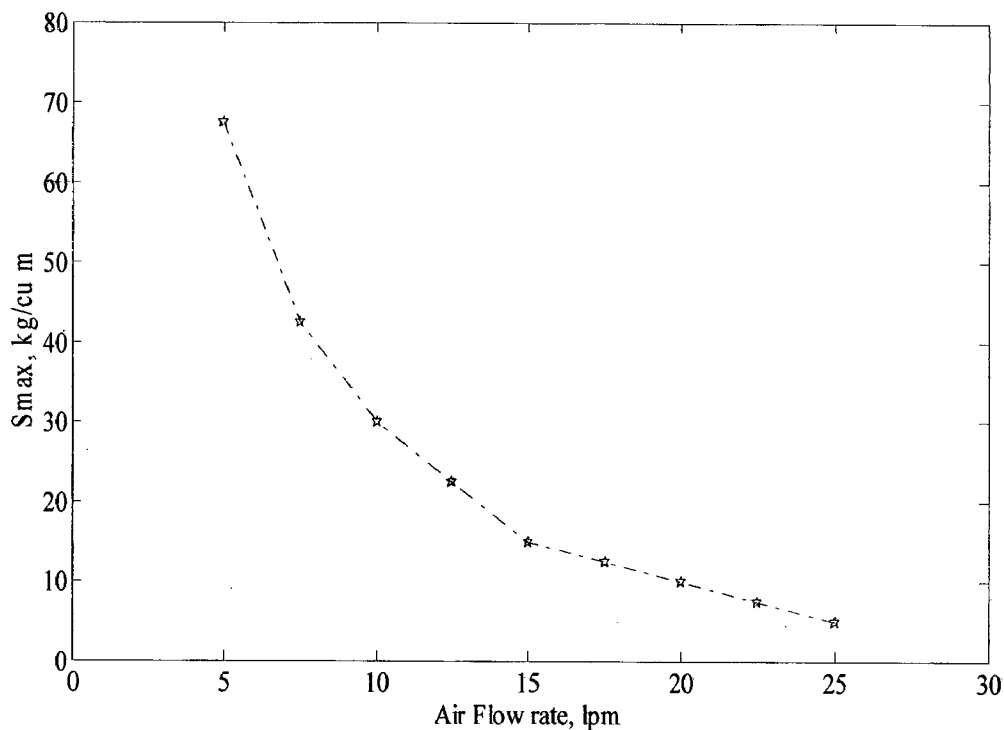


Figure 5.18 Effect of airflow rate on the substrate at 57 h of fermentation

5.4 Axial Dissolved Oxygen Profile:

Figure 5.19 shows that the dissolved oxygen profile in the riser (2–21 stages) increases because air is supplied in the riser and gas–liquid mass transfer occurs. In the riser, the interfacial mass transfer rate may be larger than the oxygen consumption of microorganisms and therefore, dissolved oxygen concentrations increased along the riser. However, the dissolved oxygen profiles decreases in the down comer (23–44 stages), in which no gas dispersion occurs and the consumption of microorganisms is higher than the

mass transfer rate. Consequently, in the down comer, oxygen is significantly consumed and as a result the dissolved oxygen concentration in the down comer decreases significantly.

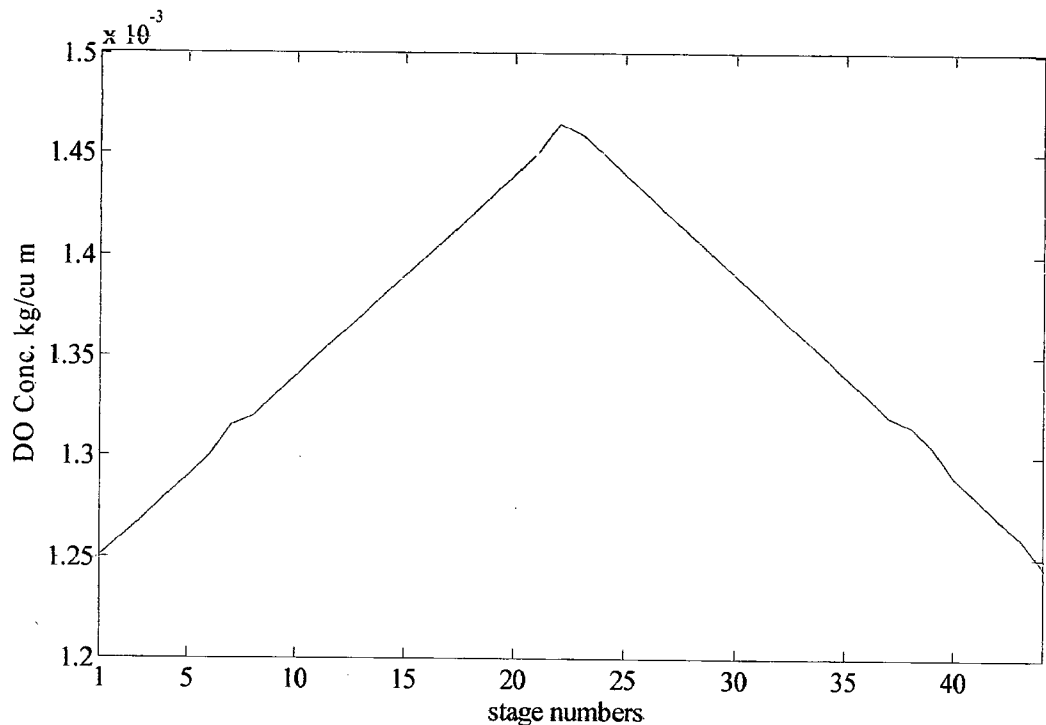


Figure 5.19 Axial variation of DO concentration in airlift bioreactor.

5.5 Effect of Number of Stages on Model Validation:

The simulation runs are carried out for different number of stages (tanks) for tanks in series model and here logistic equation is used.

Figs 5.20 through 5.22 depict the effect of number of tanks-in-series on biomass, product and substrate concentration respectively.

There is no variation in concentration profiles up to 18 h of time period. After 18 h there is small variation in concentration profiles, the maximum concentrations at 51 h are slightly lower when 22 and 30 number of stages are used as compared to values with 44 number of stages.

It can be said that for number of tanks-in-series greater than 22 there is negligible effect on steady state concentrations of biomass, product and substrate.

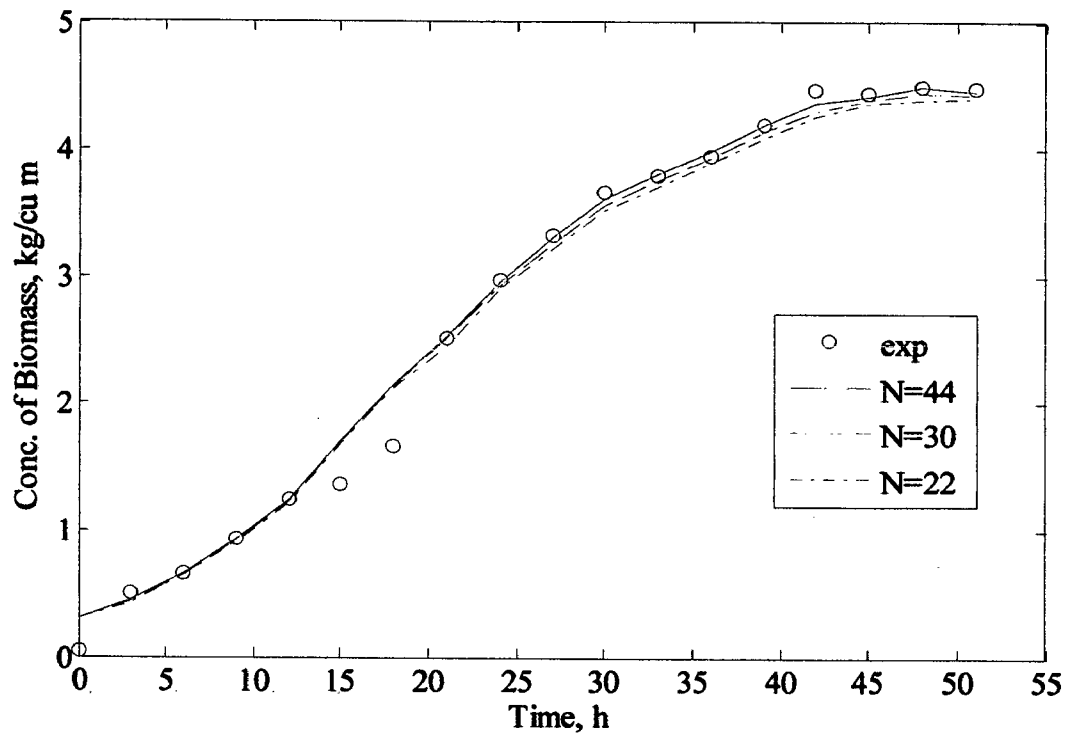


Figure 5.20 Effect of number of stages on biomass concentration profile

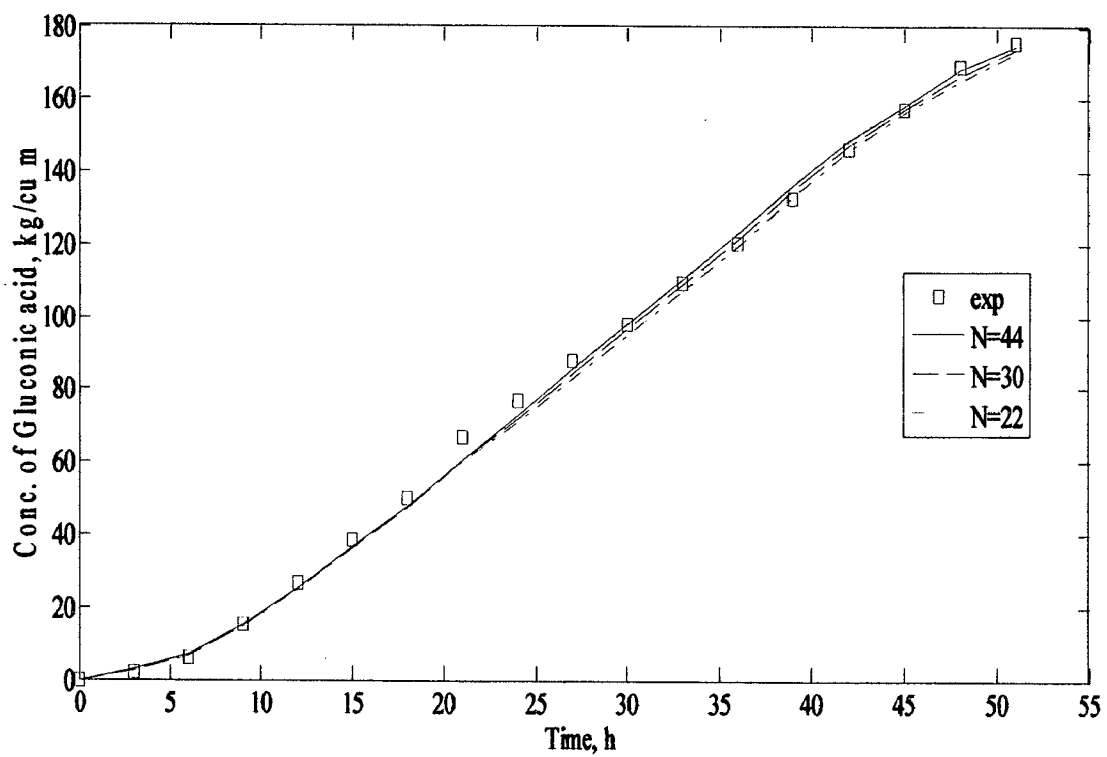


Figure 5.21 Effect of number of stages on gluconic acid concentration profile

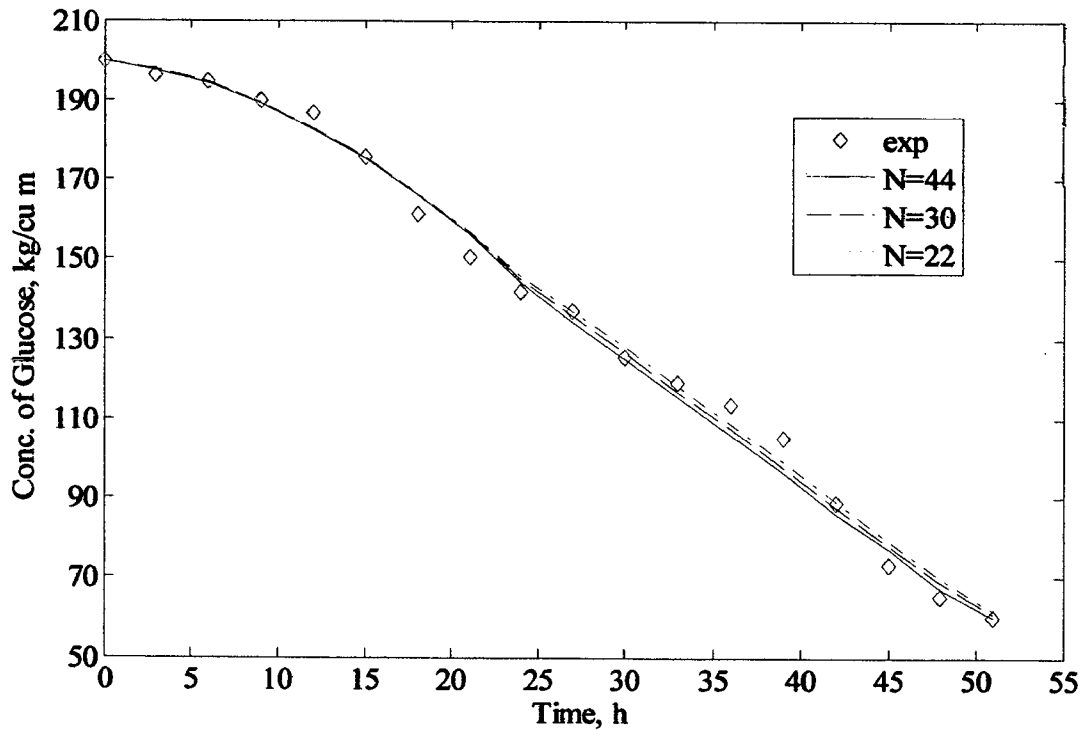


Figure 5.22 Effect of number of stages on glucose acid concentration profile

5.6 Axial Dispersion Model

5.6.1 Experimental and Predicted Biomass, GA and Substrate Concentration

Figure 5.23, 5.24 and 5.25 shows the comparison between axial dispersion model and tanks-in-series model (N=22) predictions and experimental data for biomass, GA and substrate concentrations in an ALBR. Logistic equation is used for kinetic expression. From these figures, following facts are observed.

- At higher time periods axial dispersion model slightly over predicts the concentration values in case of biomass and gluconic acid and slightly under predicts in case of glucose.
- Tanks in series model and axial dispersion model are in good agreement up to 20 h of time, deviation starts after 20 h time period. ADM concentration profile is slightly higher than the TISM concentration profile in case of biomass and gluconic acid, slightly lower than the TISM concentration profile in case of glucose.
- ADM contains in all ten ODEs and ten PDEs, time interval is taken has 3 h. For tanks-in-series N=22 has been used instead of N=44 to make computational comparable to that of ADM as it is using in all 22 sections.

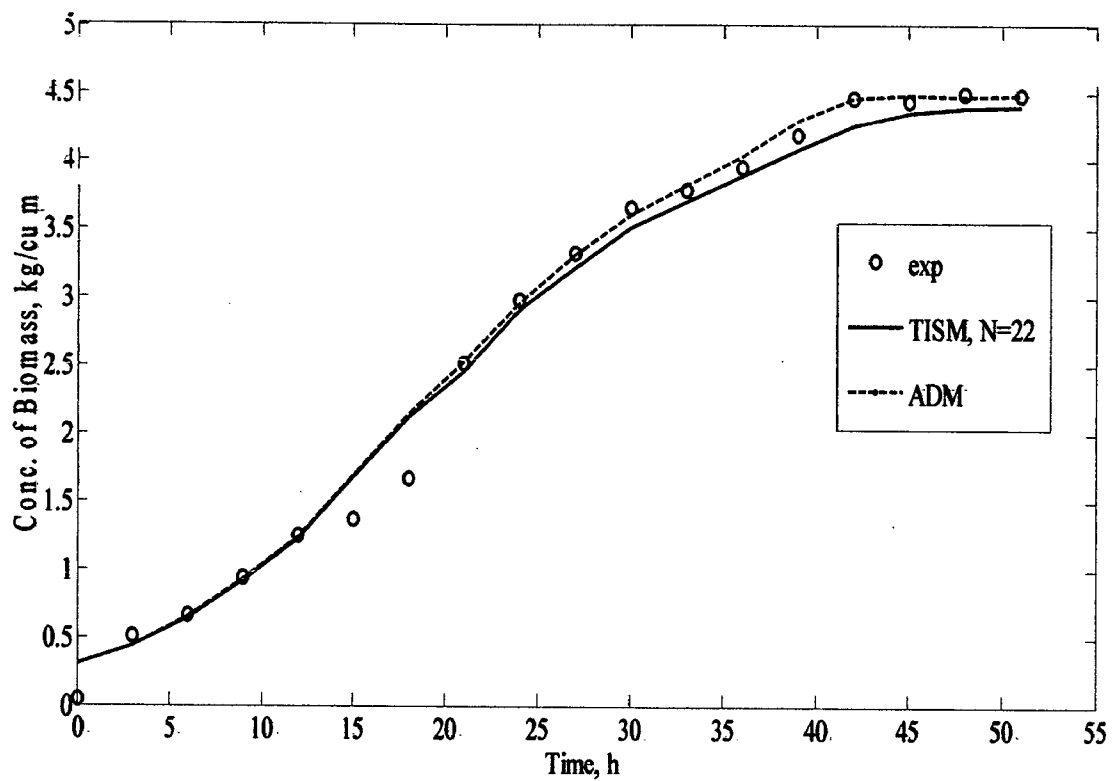


Figure 5.23 Biomass concentration profiles represented by logistic equation

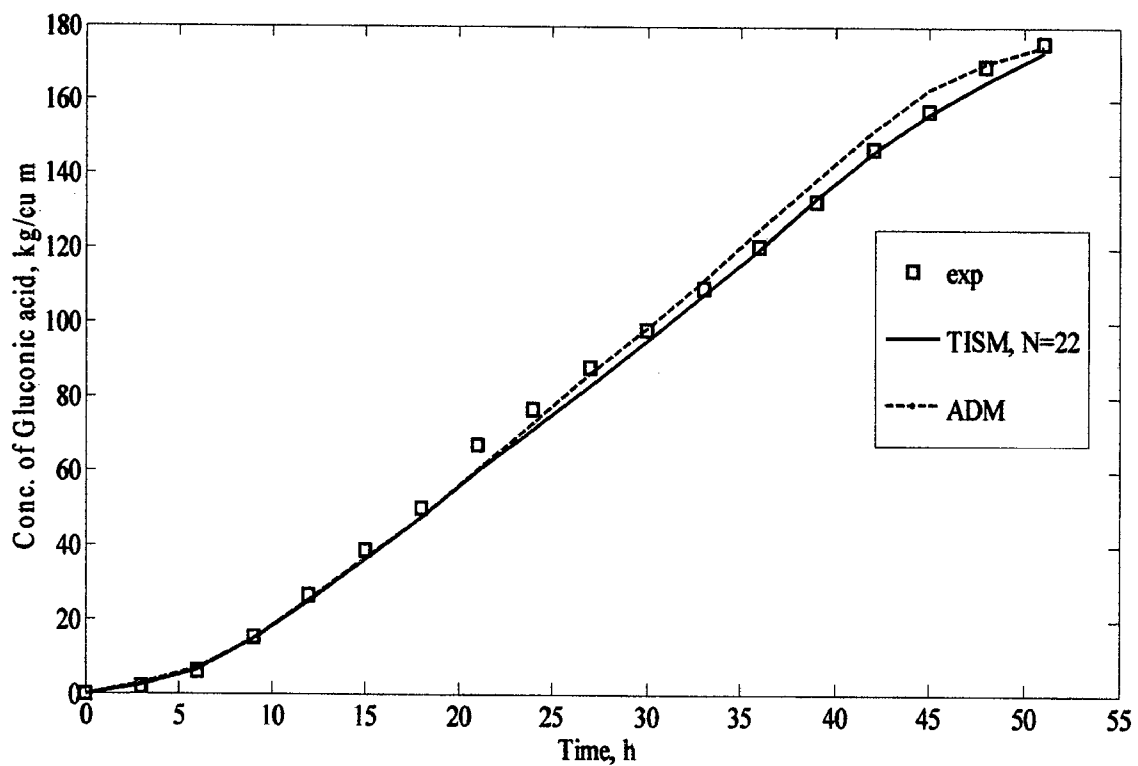


Figure 5.24 Gluconic acid concentration profiles represented by logistic equation

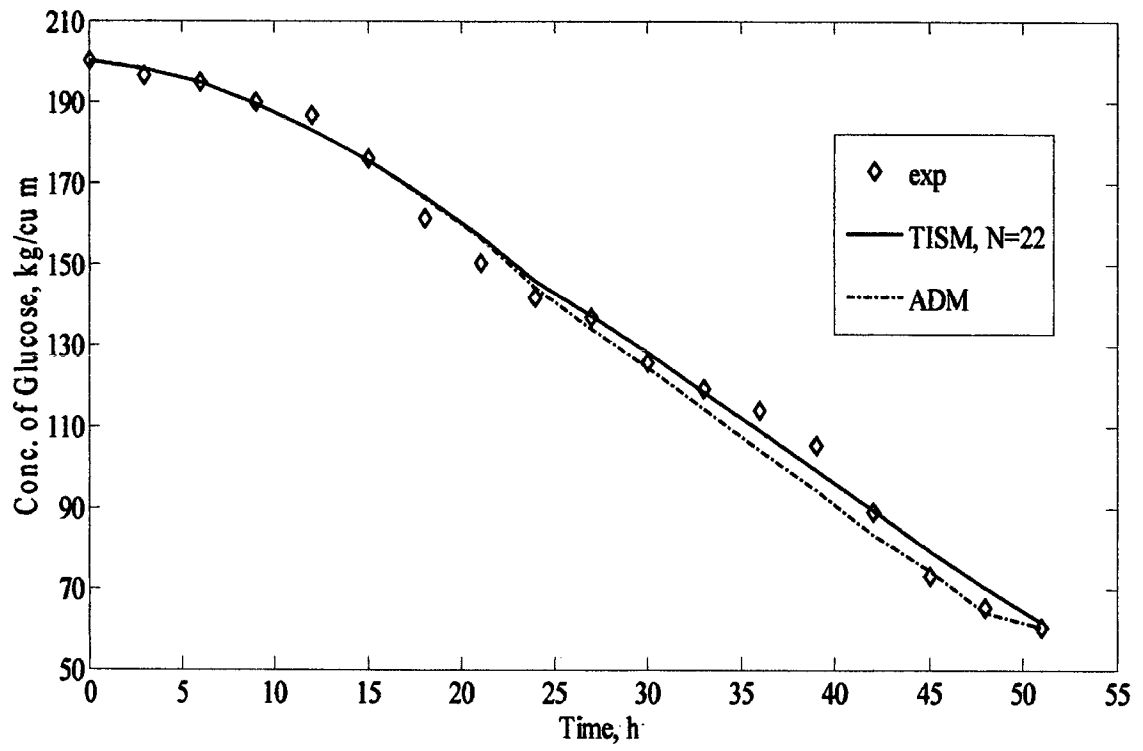


Figure 5.25 Glucose concentration profiles represented by logistic equation

Chapter-6

CONCLUSIONS AND RECOMMENDATIONS

6.1 Conclusions

Gluconic acid produced from glucose using *Aspergillus niger* is an aerobic fermentation process having two step reaction. The biotransformation represents a simple dehydrogenation reaction without involvement of complex metabolic pathways. Airlift bioreactor has been modelled by both tanks in series and axial dispersion models. These mathematical models, which incorporates two kinetic models, describes a bioprocess of gluconic acid production in batch in an airlift bioreactor (ALBR). The predictions of these models match with the experimental data. The following conclusions can be made from the results presented and discussed in previous chapter.

1. The comparison of two kinetic models, namely logistic equation and contoits model show that the logistic model represents the time dependent concentrations of biomass, gluconic acid and glucose very effectively, but fails to predict the dissolved oxygen concentration effectively. On the other hand, the contoits model predicts the time dependent dissolved oxygen concentration correctly but predicts the time dependent biomass, gluconic acid and glucose concentrations poorly.
2. The results show that the initial cell mass concentration (X_0) and airflow rate significantly affect the gluconic acid production in an airlift reactor. Higher is the initial cell mass concentration lower is the fermentation time vice versa. For gluconic acid fermentation an optimum range of airflow rate (5-20 dm³/min) is suitable in a 4.5 dm³ internal loop airlift bioreactor beyond which the process will not be economical, as it will increase operating cost without any significant improvement in product concentration.
3. Axial dissolved oxygen profile, effect of number of stages in tanks in series model has been discussed. There is no variation in concentration profiles up to 18 h of time period. After 18 h there is small variation in concentration profiles, the concentrations are slightly lower when 22 and 30 number of stages are considered compared to 44 number of stages.

4. At higher time periods axial dispersion model slightly over predicts the concentration values in case of biomass and gluconic acid, slightly under predicts in case of glucose.

6.2 Recommendations

Following future works are recommended based on the study carried out in the present work.

1. The performance of the present mathematical model can be improved by incorporating the effect of pH, temperature and inhibition of product in the basic kinetic model.
2. For further improvement of the model accuracy, more suitable correlations for the mass transfer coefficient and gas hold ups in a real fermentation system should be taken into account in the model.
3. Experimental runs should be carried out to generate more data, so that more accurate modelling can be carried out.
4. A new kinetic model can be derived which includes characteristics of logistic and contours models.
5. Different bioprocesses can be studied to check the suitability of the models for different kinetics.

REFERENCES

1. Blazej M., Kisa M. and Markos M., "Scale influence on the hydrodynamics of an internal loop airlift reactor", *Chem. Engineering and Processing*, 43, 1519-1527 (2004).
2. Boyadjiev C., "On the modeling of an airlift reactor", *International Journal of Heat and Mass Transfer*, 49, 2053–2057 (2006).
3. Chisti M.Y. and Moo-Young M., "Airlift reactors: application and design considerations", *Chemical Engineering Communications*, 60, 195-242 (1987).
4. Chisti M.Y., Choi K.H. and Moo-Young M., "Comparative evaluation of hydrodynamic and gas-liquid mass transfer characteristics in bubble column and airlift slurry reactors", *The Chemical Engineering Journal*, 62, 223-229 (1996).
5. Chisti M.Y. and Jauregui-Haza U.J., "Oxygen transfer and mixing in mechanically agitated airlift bioreactors", *Biochemical Engineering Journal*, 10, 143-153 (2002).
6. Das A. and Kundu P.N., "Microbial production of gluconic acid", *Journal of Scientific & Industrial Research*, 46, 307-331 (1987).
7. Ghose T.K., *Bioprocess Computations in Biotechnology*, Volume 1, Ellis Horwood Series in Biochemistry and Biotechnology, 302-328 (1990).
8. Ghosh P. and Ghosh T.K., "Oxygen transfer in gluconic acid fermentation", *Journal of Fermentation Technology*, 56, 139-143 (1978).
9. Hustede H., Benckiser J.A., Elves B., Hawkins S., Ravenscroft M., Rounsaville J.F., Schulz G.W., "Ullmann's Encyclopedia of Industrial Chemistry", (1989).
10. Hu-Ping L. and Al-Dahhan M., "Local characteristics of hydrodynamics in draft tube bioreactor", *Chemical Engineering Science*, 63, 3057-3068 (2008).
11. Jian-Zhong L., Weng L., Zhang Q., Xu H. and Liang-Nian J., "A mathematical model for gluconic acid production by *Aspergillus niger*", *Biochemical Engineering Journal*, 14, 137-141 (2003).
12. Jianping W., Cuiyun L., Qing Y., Xiaoqiang J., Yan S. and Wei F., "Modelling of local dynamic behavior of phenol degradation in an internal loop airlift bioreactor by yeast *candida tropicalis*", *Biotechnology & Bioengineering*, 97, 251-264 (2007).

13. Jurascik M., Blazej M., Annus J. and Markos J., "Experimental measurements of volumetric mass transfer coefficient by the dynamic pressure-step method in internal loop airlift reactors of different scale", *Chemical Engineering Journal*, 125, 81–87 (2006).
14. Kawase Y., Kanai T. and Uzumaki Y., "Simulation of airlift bioreactors: steady performance of continuous culture processes", *Computers & Chemical Engineering*, 20, 1089-1099 (1996).
15. Klein J., Rosenberg M., Markos J., Dolgos O., Kroslak M. and Kristofikova L., "Biotransformation of glucose to gluconic acid by *Aspergillus niger*—study of mass transfer in an airlift bioreactor", *Biochemical Engineering Journal*, 10, 197–205 (2002).
16. Kulkarni B.D. and Sankalp N.V., "Optimization of fermentation conditions for gluconic acid production using *Aspergillus niger* immobilized on cellulose microfibrils", *Process Biochemistry*, 37, 1343-1350 (2002).
17. Laane C., Pronk W., Franseen M. and veeger c., "Use of bioelectrochemical cell for the synthesis of (bio) chemicals", *Enzyme and Microbial Technology*, 6, 165-168 (1984).
18. Lantero O.J. and Shetty J.K., "Process for the preparation of gluconic acid and gluconic acid produced thereby", U.S. patent No. 0077062A1, April 22, 2004.
19. Levenspiel O., "The monod equation. A revisit and a generalization to product inhibition situations", *Biotechnology & Bioengineering*, 22, 1671-1687 (1980).
20. Liu J. Z., Weng L. P., Zhang O. L., Xu H. and Ji L.N., "A mathematical model for gluconic acid fermentation by *Aspergillus niger*", *Biochemical Engineering Journal*, 149, 137-141 (2003).
21. Leudking R. and Piret E.L., "A kinetic study of the lactic acid fermentation: batch process at controlled pH", *Journal of Biochemical and Microbiological Technology and Engineering*, 4, 231-241 (1959).
22. Markos J., Klein J., Rosenberg M., Dolgos O., Kroslak M. and Kristofikova L., "Biotransformation of glucose to gluconic acid by *Aspergillus niger*-study of mass transfer in an airlift reactor", *Biochemical Engineering Journal*, 10, 197-205 (2002).
23. Markos J. and Sikula I., "Modelling of enzymatic reaction in an airlift reactor using an axial dispersion model", *Chemical Papers*, 62, 10–17 (2007 a).

24. Markos J., Sikula I. and Jurascik M., "Modelling of fermentation in an internal loop airlift bioreactor", *Chemical Engineering Science*, 62, 5216 – 5221 (2007 b).
25. Morales-Barrera L. and Cristiani-Urbina E., "Removal of hexavalent chromium by *Trichoderma viride* in an airlift bioreactor", *Enzyme and Microbial Technology*, 40, 107–113 (2006).
26. Moresi M., Parante E. and Mazzatura A., "Effect of dissolved oxygen concentration on repeated production of gluconic acid by immobilised mycelia of *Aspergillus niger*", *Applied Microbiology and Biotechnology*, 36, 320-323 (1991).
27. Mukhopadhyay R., Chatterjee S., Chatterjee B.P., Banerjee P.C. and Guha A.K., "Production of gluconic acid from whey by free and immobilized *Aspergillus niger*", *International Dairy Journal*, 15, 299-303 (2005).
28. Muller and Hans-rudolf, "Process for the simultaneous production of fructose and gluconic acid from glucose-fructose mixtures", United States Patent No. 4242145, December 30, 1980.
29. Nakao K., Kiefner A., Furumoto K. and Harada T., "Production of gluconic acid with immobilized glucose oxidase in airlift reactors", *Chemical Engineering Science*, 52, 4127-4133 (1997).
30. Oosterhuis N.M.G., Groesbeek N.M., Olivier A.P.C. and Kossen N.W.F., "Scale down aspects of the gluconic acid production", *Biotechnology Letters*, 5, 141-146 (1983).
31. Park K., Pintauro P.N., Baizer M.M. and Nobe K.J., "Flow reactor studies of the paired electrooxidation and electroreduction of glucose", *Journal of Applied Electrochemistry*, 16, 1850-1855 (1986).
32. Pigache S., Trystram G. and Dhoms P., "Oxygen transfer modelling and simulation for an industrial continuous airlift fermentor", *Biotechnology & Bioengineering*, 39, 923-931 (1992).
33. Pintauro P.N., Johnson D.K., Park K., Baizer M.M., Nobe K., The paired electrochemical synthesis of sorbitol and gluconic acid in undivided flow cells", *Journal of Applied Electrochemistry*, 14, 209-220 (1984).
34. Sankpal N.V., Joshi A.P., Sutar I.I. and Kulkarni B.D., "Continuous production of Gluconic acid by *Aspergillus niger* immobilised on a cellulosic support: study of low pH fermentative behaviour of *Aspergillus niger*", *Process Biochemistry*, 35, 317-325 (1999).

35. Sankpal N.V. and Kulkarni B.D., "Optimization of fermentation conditions for gluconic acid production using *Aspergillus niger* immobilised on cellulosic microfibrils", *Process Biochemistry*, 37, 1343-1350 (2002).
36. Singh O.V., Jain R. K. and Singh R. P., "Gluconic acid production under varying fermentation conditions by *Aspergillus niger*", *Journal of Chemical Technology & Biotechnology*, 78, 208-212 (2003).
37. Singh O.V., "Production of gluconic acid from alternative economic sources", Ph.D. Thesis, Indian Institute of Technology, Roorkee, 2000.
38. Singh O.V. and Singh R.P., "Gluconic acid production by *Aspergillus niger* ORS-4.410 in submerged and solid state surface fermentation", *Indian Journal of Experimental Biology*, 39, 691-696 (2001).
39. Tokuji I., Katasho I and Mitsugi S., "Glucose Oxidase-Immobilized Benzoquinone-Mixed carbon Paste Electrode with Pre-minigrid", *Analytical Sciences*, Volume 1, 1985.
40. Tripathi C.K.M., Rastogi S., Bihari V. and Basu S.K., "production of calcium gluconate by fermentation", *Indian Journal of Experimental Biology*, 37, 731-733 (2003).
41. Van Baten J.M., Ellenberger J. and Krishna R., "Hydrodynamics of internal air-lift reactors: experiments versus CFD Simulations", *Chemical Engineering and Processing*, 42, 733-742 (2003).
42. Velizarov S. and Beschkov V., "Production of free gluconic acid by cells of *gluconobactor oxydans*", *Biotechnology letters*, 16, 407-421 (1998).
43. Vunjak-Novakovic G., Kim Y., Wu X., Berzin I. and Merchuk J.C., "Air-Lift Bioreactors for Algal Growth on Flue Gas: Mathematical Modelling and Pilot-Plant Studies", *Industrial & Engineering Chemistry Research*, 44, 6154-6163 (2005).
44. Xiaoqiang J., Jianping W., Jiang Y., Xianling L. and Feng W., "Modelling of batch phenol biodegradation in internal loop airlift bioreactor with gas recirculation by *Candida tropicalis*", *Chemical Engineering Science*, 61, 3463 – 3475 (2006).
45. Znad H., Bales V., Markos J. and Kawase Y., "Modelling and simulation of airlift bioreactors", *Biochemical Engineering Journal*, 21, 73–81 (2004 a).
46. Znad H., Blazej M., Bales V. and Markos J., "A Kinetic Model for Gluconic Acid Production by *Aspergillus niger*", *Chemical Papers*, 58, 23-28 (2004 b).

47. Znad H., Markos J. and Bales V., “production of gluconic acid from glucose by *Aspergillus niger* growth and non-growth conditions”, *Process Biochemistry*, 39, 1341-1345 (2004 c).

ANNEXURE-A

DESIGN PARAMETERS OF AIRLIFT BIOREACTOR

Recently airlift bioreactor designs have received increased attention. Due to their simple construction and less shear stress imposed on shear sensitive cells compared with stirred tanks, they have potential applications in biotechnology industries.

Mixing in ALRs is usually imperfect. From the mixing point of view, four main sections in ALRs are recognized: the bottom where the gas distributor is placed and the medium is recycled from the down comer, the riser (in the internal loop ALR (ILALR) a concentric tube), where the medium flows upward, the gas separator and the down comer.

The airlift reactor is a promising reactor for two and three phase reactions due its advantages of high fluid circulation, heat and mass transfer, short mixing time, low shear stress and low energy consumption. Airlift reactors have been widely applied in chemical engineering, biochemical fermentation and biological waste water treatment processes. In order to design such a bioreactor with confidence, further information is required on the relationship between its performance and hydrodynamic, heat and mass transfer characteristics.

A.1 Design Details of Internal Loop Airlift Bioreactor

An airlift reactor consists of four distinct sections: riser, down comer, top and bottom sections. Each section of ALR exhibits different hydrodynamic and mixing behaviour. Airlift reactors have no moving parts and mixing is caused pneumatically. Gas-liquid circulation is caused by the gradient in density between riser and down comer because the gas hold up is different in riser and down comer.

The main specifications of the reactor are:

Draft tube (Riser tube) : ID = 0.042 m, Height = 100 cm

Airlift reactor tube (Down comer) : ID = 0.0725 m, Height = 1.032 m

Separator : ID = 0.2 m, Height = 0.18 m

Bottom section : ID = 0.0725 m, Height = 0.03m

Upper and lower parts of reactor are made of SS 304, whereas middle parts including riser and down comer sections are made of glass for visualization of mixing. Entire stand was made from SS 304 and glass bottles are placed at the top for addition of base, acid or antifoam etc. The working volume of the reactor is 4.5 dm^3 .

The overall size of the experiment set-up made of SS and glass is about $2\text{m} \times 1\text{m}$. The system is closed and designed such that it can be sterilized in situ using steam at about 121°C for 15 min after replacing sensors and probes by blinds. Sparger can also be removed for cleaning purpose and replaced by another one to sparge in down comer. Water-cooling is provided to maintain the temperature of the system by manually controlling the flow rate. The size of the air filters provided at the inlet and outlet has pore size of $0.2 \mu\text{m}$, which prevents entry of any microbes present in the atmospheric air.

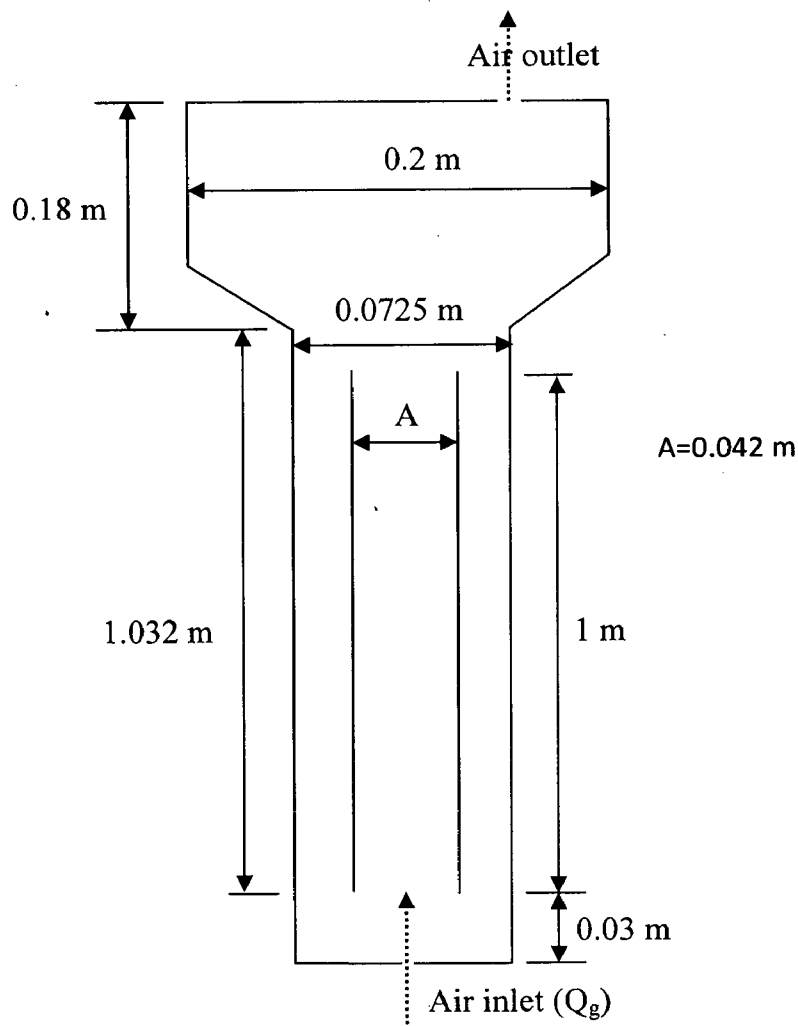


Fig A.1 Schematic diagram of experimental set up with dimension

ANNEXURE-B

Table B.1 Experimental data of bioprocess for gluconic acid production Znad et al. (2004)

Sl. No.	Time (hour)	Biomass Concentration (kg/m ³)	Gluconic acid Concentration (kg/m ³)	Glucose Concentration (kg/m ³)	DO Concentration (kg/m ³)
1	0	0.04	0	200	0.0065
2	3	0.503	1.96	196.302	0.0058
3	6	0.662	6.23	194.66	0.0045
4	9	0.939	15.4	189.789	0.0041
5	12	1.247	26.68	186.532	0.0035
6	15	1.366	38.686	175.746	0.0028
7	18	1.661	49.975	161.194	0.0025
8	21	2.511	66.91	150.405	0.0024
9	24	2.973	76.788	141.771	0.0024
10	27	3.324	88.078	136.9	0.0023
11	30	3.656	97.956	125.576	0.0022
12	33	3.786	109.245	119.092	0.002
13	36	3.952	120.535	113.681	0.0019
14	39	4.192	132.53	105.274	0.0019
15	42	4.469	146.642	88.88	0.0018
16	45	4.44	157.226	73.252	0.0018
17	48	4.502	169.22	65.155	0.0017
18	51	4.488	175.57	60.284	0.0017

Table B.2 Simulation data for gluconic acid production by tanks in series model using logistic equation

Sl. No.	Time (hour)	Biomass Concentration (kg/m ³)	Gluconic acid Concentration (kg/m ³)	Glucose Concentration (kg/m ³)	DO Concentration (kg/m ³)
1	0	0.3080	0	200.0000	0.0065
2	3	0.4501	2.7834	197.5647	0.0059
3	6	0.6612	6.9712	194.3220	0.0054
4	9	0.9294	15.2378	189.0214	0.0049
5	12	1.2452	25.5155	182.2986	0.0044
6	15	1.7018	36.6209	175.2112	0.0038
7	18	2.1496	47.7261	165.8669	0.0033
8	21	2.5243	60.5507	156.2344	0.0030
9	24	2.9537	72.6440	144.2116	0.0027
10	27	3.3122	85.7241	134.1338	0.0025
11	30	3.6120	97.9567	125.0653	0.0023
12	33	3.8068	110.3450	115.3229	0.0021
13	36	3.9923	122.9521	105.9016	0.0019
14	39	4.1926	136.3516	96.2114	0.0018
15	42	4.3620	148.6528	86.1920	0.0018
16	45	4.4144	158.3559	77.2116	0.0018
17	48	4.4926	168.2432	67.2119	0.0017
18	51	4.4551	174.5743	60.1720	0.0017

Table B.3 Simulation data for gluconic acid production by tanks in series model using
contois equation

Sl. No.	Time (hour)	Biomass Concentration (kg/m ³)	Gluconic acid Concentration (kg/m ³)	Glucose Concentration (kg/m ³)	DO Concentration (kg/m ³)
1	0	0.0400	0	200.0000	0.0065
2	3	0.1051	1.8821	198.1449	0.0055
3	6	0.2454	5.0040	197.2341	0.0048
4	9	0.5010	6.9281	194.2337	0.0041
5	12	0.8245	9.7846	192.0449	0.0035
6	15	1.3559	15.6782	187.1120	0.0030
7	18	1.6847	25.5243	182.2232	0.0026
8	21	2.1944	33.6239	175.1218	0.0024
9	24	2.6546	45.0469	165.4334	0.0023
10	27	3.0047	60.0463	155.5433	0.0022
11	30	3.4041	74.6591	145.0127	0.0021
12	33	3.7069	94.2528	135.0016	0.0020
13	36	3.9120	112.1246	120.1124	0.0019
14	39	4.2045	130.6824	106.1170	0.0018
15	42	4.4790	145.5929	90.7661	0.0017
16	45	4.7528	163.6582	75.2437	0.0017
17	48	5.0126	182.9812	64.2218	0.0017
18	51	5.2043	192.9720	50.0124	0.0017

Table B.4 Effect of initial biomass concentration (X_0) on biomass growth

Sl. No.	Time (hour)	Biomass Concentration (kg/m ³)	Biomass Concentration (kg/m ³)	Biomass Concentration (kg/m ³)	Biomass Concentration (kg/m ³)
		$X_0=0.10472$	$X_0=0.20636$	$X_0=0.40964$	$X_0=0.51128$
1	0	0.1047	0.2063	0.4096	0.5112
2	3	0.2033	0.3083	0.5612	0.7349
3	6	0.2081	0.4426	0.8349	1.1540
4	9	0.3563	0.6248	1.2541	1.5525
5	12	0.5069	0.7829	1.5525	1.9547
6	15	0.7126	1.1246	2.0026	2.3828
7	18	1.0118	1.4428	2.4752	2.8124
8	21	1.2125	1.7529	2.7758	3.2125
9	24	1.5529	2.2124	3.2249	3.5547
10	27	2.0553	2.5561	3.5040	3.8120
11	30	2.5126	2.8550	3.8124	4.0542
12	33	2.8567	3.3129	4.0542	4.3124
13	36	3.2123	3.4560	4.2548	4.4926
14	39	3.4549	3.8518	4.3549	4.6127
15	42	3.8120	4.0125	4.4544	4.6820
16	45	4.0521	4.2526	4.5015	4.6831
17	48	4.25430	4.3781	4.5257	4.6824
18	51	4.3672	4.4125	4.5291	4.6795

Table B.5 Effect of initial biomass concentration (X_0) on gluconic acid production.

Sl. No.	Time (hour)	Gluconic acid Concentration (kg/m^3)	Gluconic acid Concentration (kg/m^3)	Gluconic acid Concentration (kg/m^3)	Gluconic acid Concentration (kg/m^3)
		$X_0=0.10472$	$X_0=0.20636$	$X_0=0.40964$	$X_0=0.51128$
1	0	0	0	0	0
2	3	2.0031	2.0531	6.4821	8.4781
3	6	3.5723	5.0289	13.2463	18.5723
4	9	6.9818	10.2350	22.5869	30.2790
5	12	10.2394	20.2156	34.6403	40.0150
6	15	15.9746	28.5781	45.0440	51.2843
7	18	22.5261	35.5119	54.7849	63.7851
8	21	32.5598	45.0102	70.5689	78.9732
9	24	40.5765	58.7503	82.4854	90.8969
10	27	55.5291	72.5130	95.2753	105.2487
11	30	65.5703	85.0181	109.3407	118.1445
12	33	80.5261	97.5271	120.9731	131.2727
13	36	90.2489	110.5239	135.5729	142.0218
14	39	103.3961	121.5701	145.4438	150.2722
15	42	116.6827	136.5283	156.9771	160.2817
16	45	132.7590	148.6524	164.8402	170.4645
17	48	150.0212	158.3557	172.4431	177.8863
18	51	165.2354	170.5223	176.5820	181.1120

Table B.6 Effect of initial biomass concentration (X_0) on glucose consumption

Sl. No.	Time (hour)	Glucose Concentration (kg/m^3)	Glucose Concentration (kg/m^3)	Glucose Concentration (kg/m^3)	Glucose Concentration (kg/m^3)
		$X_0=0.10472$	$X_0=0.20636$	$X_0=0.40964$	$X_0=0.51128$
1	0	200.0000	200.0000	200.0000	200.0000
2	3	199.8534	198.8949	195.9534	194.0534
3	6	198.8531	196.2328	192.3921	190.5521
4	9	196.7567	194.3483	185.5780	182.5589
5	12	194.8990	190.0521	178.6827	175.0464
6	15	190.5543	182.5646	170.9834	165.8109
7	18	182.5912	176.7897	162.8154	157.5836
8	21	176.8850	166.5325	152.9901	146.8943
9	24	168.5528	158.3493	140.8124	136.8894
10	27	160.9815	148.3428	128.8934	123.5718
11	30	150.5516	135.0320	120.8818	114.5730
12	33	137.8645	125.2891	110.8950	105.7845
13	36	126.5517	116.8913	102.7732	96.8932
14	39	116.3453	107.3415	90.5832	86.7890
15	42	106.0528	97.0294	81.8834	78.8813
16	45	95.3456	83.2653	74.55790	70.9810
17	48	78.5459	72.3642	66.5554	64.7855
18	51	64.5514	62.3451	58.7523	56.8977

Table B.7 Effect of airflow rate on the biomass, gluconic acid and substrate concentrations at 57 h of fermentation

Sl. No.	Qg (dm ³ .min-1)	Xmax (g/dm ³)	Pmax, (g/dm ³)	Smax, (g/dm ³)
1	5	3.8513	162.5478	67.5074
2	7.5	4.6024	185.0735	42.5145
3	10	5.1548	200.0032	30.6426
4	12.5	5.6040	212.5478	22.5367
5	15	5.8513	222.5419	15.2057
6	17.5	6.0211	230.0895	12.5189
7	20	6.0919	235.2834	10.0711
8	22.5	6.1462	237.5143	7.5321
9	25	6.1657	240.1032	5.3401

Table B.8 Simulation data for gluconic acid production by axial dispersion model using logistic equation

Sl. No.	Time (hour)	Biomass Concentration (kg/m ³)	Gluconic acid Concentration (kg/m ³)	Glucose Concentration (kg/m ³)
1	0	0.3080	0	200.0000
2	3	0.4401	2.5843	197.7652
3	6	0.6501	6.7761	194.5446
4	9	0.9193	15.0378	189.2348
5	12	1.2325	25.2569	182.6734
6	15	1.6885	36.3710	175.4481
7	18	2.1365	47.4705	166.0133
8	21	2.5214	60.5133	156.1347
9	24	2.9546	72.9861	143.9220
10	27	3.3112	86.1331	133.7212
11	30	3.6128	98.5519	124.5784
12	33	3.8269	111.4554	114.2225
13	36	4.0421	124.9839	103.8898
14	39	4.2963	138.4532	94.1214
15	42	4.4690	151.7649	83.0923
16	45	4.4892	162.9871	74.1927
17	48	4.4863	170.3425	64.1018
18	51	4.4894	174.9808	60.2669

Table B.9 Effect of number of stages in tanks in series model on biomass, gluconic acid and substrate concentrations

Sl. No.	Time (hour)	Biomass Concentration (kg/m ³)		Gluconic acid Concentration (kg/m ³)		Glucose Concentration (kg/m ³)	
		N=22	N=30	N=22	N=30	N=22	N=30
1	0	0.3080	0.3080	0	0	200.0000	200.0000
2	3	0.4313	0.4439	2.3845	2.5846	197.9640	197.7645
3	6	0.6415	0.6519	6.5760	6.7791	194.7228	194.5223
4	9	0.9093	0.9195	14.8371	15.0308	189.4217	189.2218
5	12	1.2278	1.2325	25.0145	25.2564	182.7984	182.5485
6	15	1.6769	1.6885	36.1267	36.3754	175.7112	175.4619
7	18	2.1247	2.1365	47.2259	47.4765	166.3665	166.1164
8	21	2.4490	2.5115	60.0530	60.3113	156.7347	156.4840
9	24	2.9036	2.9284	71.1659	71.8958	145.7114	144.9615
10	27	3.2128	3.2623	82.7248	84.2267	137.1339	135.6338
11	30	3.5124	3.5625	94.9563	96.4565	128.0650	126.5659
12	33	3.7061	3.7569	107.3452	108.8459	118.3225	116.8224
13	36	3.8927	3.9420	119.5676	121.4541	108.9014	107.4013
14	39	4.0925	4.1423	133.3598	134.8510	99.2117	97.7112
15	42	4.2646	4.3026	145.7650	147.1528	89.1929	87.6928
16	45	4.3647	4.3895	156.3451	157.3019	79.2115	78.2116
17	48	4.3925	4.4423	165.198	166.7425	70.2117	68.7115
18	51	4.4052	4.4390	173.081	173.8232	61.6728	60.9224